

CONFIDENTIAL

Copy 5
RM L53E12

UNCLASSIFIED

NACA RM L53E12



RESEARCH MEMORANDUM

EFFECTS OF COMPRESSIBILITY AT MACH
NUMBERS UP TO 0.8 ON INTERNAL-FLOW CHARACTERISTICS
OF A COWLING-SPINNER COMBINATION EQUIPPED WITH AN
EIGHT-BLADE DUAL-ROTATION PROPELLER

By Gene J. Bingham and Arvid L. Keith, Jr.

Langley Aeronautical Laboratory
Langley Field, Va.

CLASSIFICATION CANCELLED

Auth: *NACA R72785* Date: *10/12/54*

By: *msa 11/9/54* See _____ CLASSIFIED DOCUMENT

This material contains information affecting the National Defense of the United States within the meaning of the espionage laws, Title 18, U.S.C., Secs. 793 and 794, the transmission or revelation of which in any manner to an unauthorized person is prohibited by law.

NATIONAL ADVISORY COMMITTEE FOR AERONAUTICS

WASHINGTON

June 26, 1953

UNCLASSIFIED

CONFIDENTIAL



NATIONAL ADVISORY COMMITTEE FOR AERONAUTICS

RESEARCH MEMORANDUM

EFFECTS OF COMPRESSIBILITY AT MACH
NUMBERS UP TO 0.8 ON INTERNAL-FLOW CHARACTERISTICS
OF A COWLING-SPINNER COMBINATION EQUIPPED WITH AN
EIGHT-BLADE DUAL-ROTATION PROPELLER

By Gene J. Bingham and Arvid L. Keith, Jr.

SUMMARY

An investigation has been conducted at Mach numbers up to 0.8 for the purpose of studying the effects of compressibility on the internal-flow characteristics of an NACA 1-series cowling-spinner combination (D-type), equipped with a dual-rotation propeller. Two 24-percent-thick shank propellers were investigated; one had a sealed propeller-spinner juncture and the other had a raised-platform-airfoil shaped juncture. A brief investigation was also made at a low-speed free-stream Mach number (0.30) in order to study the effects of variations in inlet height and rate of internal compression on the internal-flow characteristics with propeller removed. The results of the main part of the investigation indicate that the propeller had no appreciable compressibility effects on the impact pressures when operating at the design cruise blade angle. With increases in shank loading, however, shock and shock-boundary-layer-interaction effects caused reductions in impact pressure at a Mach number of 0.8. Installation of the platform-type propeller-spinner-juncture configuration investigated with a blade-platform gap height of 0.020 inch (approximately 1/8 inch full scale) caused a reduction in inlet impact pressure coefficient of about 4 percent for the propeller design cruise blade angle. The results of the low-speed portion of the investigation indicate that the inlet height (as low as $0.055D_c$ where D_c is maximum diameter of cowling) and rate of internal compression has no significant effect on the inlet-velocity ratio at which separation from the spinner occurs.

INTRODUCTION

The development of basic design data for NACA 1-series cowling-spinner combinations (D-type cowling) is reported in reference 1. In

~~CONFIDENTIAL~~

UNCLASSIFIED

order to investigate the possibility of direct application of these data to a gas turbine-propeller installation, the effects of propeller-shank thickness and propeller-spinner-juncture configuration on the internal-flow characteristics of a cowling-spinner combination equipped with an eight-blade dual-rotation propeller have been investigated at low speed and the results reported in reference 2. Further studies of the effects of propeller-spinner-juncture configuration (ref. 3) on the pressure recovery of this type cowling with a four-blade single-rotation propeller have been made at Mach numbers up to 0.83.

The purpose of the present investigation was to study the effects of compressibility at Mach numbers up to 0.8 on the internal-flow characteristics of a cowling-spinner configuration in combination with a dual-rotation propeller. In effect, this study was an extension of the previous low-speed investigation (ref. 2) in that the basic inlet and spinner dimensions remained the same and two of the propeller-juncture configurations studied therein were investigated.

For the main part of the tests, which were conducted in the Langley low-turbulence pressure tunnel, the basic cowling-spinner combination was studied with propeller removed and with two propeller configurations installed. The two propeller configurations were similar in that they had the same blade form and plan form. The shanks of one propeller were extended to the spinner surface and sealed; the other had a raised-platform-type juncture with the gap required to allow blade-angle changes located outside of the spinner boundary layer. Several low-speed tests were also made with three additional cowling configurations to determine the effects of inlet height and rate of internal compression on the inlet-velocity ratio at which flow separation from the spinner surface occurs. The internal-flow characteristics were determined by total- and static-pressure surveys at the inlet and diffuser stations and the internal-flow rate was measured at a venturi station.

SYMBOLS

A	area
b	blade chord
d	inlet diameter
D	maximum diameter
h	normal distance from central body

h' blade thickness

H total pressure

M Mach number

n propeller rotational speed

p static pressure

$\frac{p - p_0}{H_0 - p_0}$ static-pressure coefficient

$\frac{H - p_0}{H_0 - p_0}$ impact (total) pressure coefficient

$\left(\frac{H - p_0}{H_0 - p_0}\right)_{av}$ average weighted impact pressure coefficient,

$$\frac{\int_{0^\circ}^{360^\circ} \int_{r_B}^{r_C} \frac{H - p_0}{H_0 - p_0} \frac{\rho V}{\rho_0 V_0} r \, dr \, d\theta}{\int_{0^\circ}^{360^\circ} \int_{r_B}^{r_C} \frac{\rho V}{\rho_0 V_0} r \, dr \, d\theta}$$

q dynamic pressure

V velocity

V/nD propeller advance ratio

R maximum radius

r radius from cowling center line

x distance from leading edge of propeller, spinner, or cowling

X maximum length of component

Y maximum ordinate of component

z land height above spinner surface normal to axis

α	angle of attack of center line of model
β	angle of attack of propeller blades from plane of rotation (blade-angle values given herein at $(r/R)_p = 0.75$)
δ	nominal boundary-layer thickness (defined as normal distance from surface to point where $\frac{H - P_0}{H_0 - P_0} = 0.95$)
θ	radial rake station measured clockwise from top of model looking downstream
c_{ld}	blade section design lift coefficient

Subscripts:

av	average
c	cowling
s	spinner or central body
l	inlet
d	diffuser or design value
o	free stream
F	front blade
R	rear blade
p	propeller

MODEL

A plan-form drawing of the model is presented in figure 1 and photographs of the model are shown in figure 2. The basic configuration consists of an NACA 1-series cowling-spinner combination (D-type) mounted on a ducted body of revolution which was supported in the 3- by $7\frac{1}{2}$ -foot rectangular test section of the Langley low-turbulence pressure tunnel by an airfoil strut. The cowling diameter (10.8 inches) was determined to be the maximum that would permit choke-free tunnel operation up to a test Mach number of 0.8.

Spinner.- The NACA 1-51.6-094.4 spinner ($D_S/D_C = 0.516$; $X_S/D_C = 0.944$) was selected as being the shortest length, smallest diameter, 1-series spinner that would enclose a representative hub and blade-angle-change mechanism for an eight-blade dual-rotation propeller. The over-all spinner dimensions were the same as those of reference 2 and the division between the counterrotating portions, for the propeller-installed case, was made at $x/X_S = 0.609$; the gap between spinner components was 0.03 inch. For the propeller-removed test the spinner gaps were sealed.

Cowlings.- The NACA 1-69.8-077.7 cowling ($d/D_C = 0.698$; $X_C/D_C = 0.777$), herein referred to as "basic cowling," was selected by the method of reference 1 to fulfill the air-flow requirements of a representative turbo-propeller engine producing about 5,500 horsepower when operating at a cruise Mach number of 0.8 with an inlet-velocity ratio of 0.5 at an altitude of 35,000 feet. An NACA 1-series inner liner ($Y = 0.01D_C$; $X = 0.04D_C$) was used, as recommended in reference 1, to aid in the avoidance of flow separation from the inner lip when operating at high inlet-velocity ratios or at high angles of attack. The internal ducting also included a 4.38° equivalent conical diffuser with an area ratio A_d/A_1 of 1.4 where $A_1 = 18.6$ square inches.

Three additional cowlings were also studied. The first was similar to the basic cowling with the exception that it had no internal diffuser ($A_d/A_1 = 1.0$). The other two were the NACA 1-75.6-077.7 cowling with no diffuser ($A_1 = 26.04$ square inches) and the NACA 1-63.8-077.7 cowling with an 8.76° equivalent conical diffuser ($A_d/A_1 = 2.26$ where $A_1 = 11.54$ square inches). Each of the additional cowlings had the same NACA 1-series inner liner as the basic cowling. Internal area distributions and a sketch of the spinner and cowlings tested are shown in figure 3. Station 0 for each cowling was fixed at the same station of the spinner (at the position shown by the NACA 1-69.8-077.7 cowling in fig. 3).

Propeller and propeller-spinner junctures.- Plan-form and blade-form curves of the test propeller are shown in figure 4. The propeller was composed of NACA 16-series airfoil sections and was designed to operate at an advance-diameter ratio of 4.2 at a cruise Mach number of 0.8 in accordance with the design considerations of reference 4. The root blade thickness h'/b was 0.24 at the spinner surface; blade angles at the spinner surface for the front and rear blades were 85.6° and 82.8° , respectively.

Two types of propeller-spinner junctures were investigated. The first, designated ideal juncture, had the shank-spinner gap sealed and faired into the spinner surface; the other had a raised-platform-type juncture (fig. 5) which located the gap required to allow changes in blade angle outside of the spinner boundary layer. This juncture was

the most efficient practical juncture investigated in the low-speed test reported in reference 2. The platform was fixed at the design cruise blade angle with a junction gap of 0.020 inch. Considerations leading to the choice of this gap height are discussed in a subsequent section.

APPARATUS AND TESTS

Measurements of pressure distributions were made at the inlet and diffuser stations and the internal mass-flow rate, which was regulated by a movable tail plug, was determined at the venturi. Unpublished data, obtained during the low-speed test of reference 2, indicated that the flow angularity behind these blades did not necessitate the use of shielded pressure tubes. The model measuring stations are shown in figure 1 and the tube arrangements are given in the following table. (The inlet rakes were removed when diffuser measurements were being made.)

NACA cowling	Measuring station	Number of tubes per rake		Number of surface orifices per rake	Rake positions, θ , deg
		Total pressure	Static pressure		
1-69.8-077.7 (Basic cowling)	Inlet	8	1	2	0, 135, 180, 270, and 315
	Diffuser	10	1	2	0, 135, 180, 270, and 315
1-69.8-077.7 ($A_d/A_1 = 1.0$)	Inlet	8	1	2	0, 135, 180, 270, and 315
	Diffuser	8	1	2	0, 135, 180, 270, and 315
1-63.8-077.7	Inlet	6	1	2	0, 135, 180, 270, and 315
	Diffuser	10	1	2	0, 135, 180, 270, and 315
1-75.6-077.7	Inlet	10	1	2	0, 135, 180, 270, and 315
	Diffuser	10	1	2	0, 135, 180, 270, and 315
-----	Venturi	5	1	1	0, 45, 90, 105, 180, 225, and 270

The static orifices in the central body and inner cowling surfaces were located 1 tube diameter (0.050 inch) ahead of the plane of the total-pressure rakes and these tube readings may have been influenced by the pressure field of the rake. Determinations of inlet-velocity ratios by use of all the inlet-pressure tubes, however, checked within ± 0.01 of that obtained at the venturi station for separation-free conditions. The average weighted impact pressure coefficients and the inlet mass-flow ratios were integrated by the use of Simpson's Rule with the following assumption made with regard to pressure (see preceding table): at inlet and diffuser radius rake station, 45° same as 315° , 90° same as 270° , and 225° same as 135° ; at venturi radius rake station, 315° same as 45° .

Comparisons of the average impact pressure coefficients of the present study at the lowest test speeds and those presented in reference 2 for the same spinner-inlet and propeller components will show discrepancies especially for inlet-velocity ratios where flow separation occurred ahead of the measuring station. Such discrepancies are attributed mainly to differences in pressure-tube instrumentation. The total-pressure-tube instrumentation used in reference 2 consisted of only one rake of tubes installed in the inlet and diffuser at the top vertical center line, whereas the present test configuration has five total- and static-pressure tube rakes distributed around the annulus of the inlet and diffuser with each rake more adequately covering each annulus station.

The eight-blade counterrotating propeller was driven by a 60-horsepower induction motor and the power was transmitted through a 3-to-1 gear reduction drive (fig. 1). Because of the drive power limitations and the test-section width, each propeller was cut off at the 45.9-percent-radius station and the tips were rounded; the advance ratios presented, however, are based on the full-scale model diameter of 3.09 feet. A preliminary investigation showed that reducing the model propeller diameter which was used for the test of reference 2 to the present value of $r/R = 0.459$ had no significant effects on the internal-flow characteristics.

Tests were conducted over a range of inlet-velocity ratio from approximately 0.2 to 1.0 for the following test conditions:

Configuration	Blade angle, deg	α , deg	V/nD	M_0
Propeller removed	-----	0, 2.5, and 5	----	0.3 to 0.8
Propeller installed (tested with basic cowling only)	Cruise: $\beta_F = 63.1$	^a 0, 2.5, and 5	^b 4.2 3.5	0.6 to 0.8
	$\beta_R = 62.3$	^c 0	4.2 3.5	0.6 to 0.8
	High speed: $\beta_F = 67.4$	^a 0, 2.5, and 5	^b 5.25 4.2	0.6 to 0.8
	$\beta_R = 66.6$	^c 0	^b 5.25 4.2	0.6 to 0.8

^aIdeal juncture

^bAssumed operational values

^cPlatform juncture

Both air, at atmospheric pressure, and Freon-12, at a stagnation pressure of 10 inches of mercury absolute, were used as testing mediums. The resulting Reynolds numbers were 1.92×10^6 for air ($M_0 = 0.3$), and ranged from 2.60×10^6 to 3.05×10^6 for Freon-12 ($M_0 = 0.6$ to 0.8) based on a maximum cowling diameter of 10.8 inches. The data obtained in Freon-12 are presented as corresponding values in air. The conversion from Freon-12 to air was based on the streamline similarity concept discussed in reference 5 and was almost negligible for most of the parameters measured in the present investigation up to the maximum test Mach number of 0.8.

RESULTS AND DISCUSSION

Basic configuration, propeller removed.- Typical total- and static-pressure distributions at the five inlet- and diffuser-rake stations of the basic cowling-spinner combination are shown in figure 6 for angles of attack of 0° and 5° ($M_0 = 0.68$). Near-stream impact pressure is indicated over the annulus at the high inlet-velocity ratios with the exception of the regions affected by skin-friction losses. As the inlet-velocity ratio was reduced, the boundary layer thickened and finally separated because of the adverse pressure rise of the internal-flow system. At 0° angle of attack the distributions also show that

flow asymmetry began to occur at the inlet for the lower inlet-velocity ratios. It was noted during the test that, under these conditions, the flow surged alternately from one position to another.

The effect of increasing the angle of attack to 5° (figs. 6(c) and 6(d)) was to thin out the boundary layer at the bottom of the inlet for the entire test range and to require a higher inlet-velocity ratio for the avoidance of separation from the top of the spinner. At an inlet-velocity ratio of approximately 0.4 and below, the inlet pressure distributions indicate that the flow in the top portion of the inlet was reversed and that the separated air spilled above the inlet. For these conditions, the internal flow moved up and around the central body and the local impact pressure coefficients were higher in the top portion of the diffuser than for the 0° angle-of-attack case. As the inlet-velocity ratio was increased, separated flow began to enter the top portion of the inlet and the pressures in the top portion of the diffuser were progressively reduced over a small range of V_1/V_0 . With further increases in inlet-velocity ratio, separation was eliminated ahead of the inlet and the diffuser local impact pressure coefficient began to increase. It will be noted that the NACA 1-series inner liner used in this case was sufficient to avoid separation from the inlet lip for all test conditions.

The effects of inlet-velocity ratio and angle of attack on the internal pressure recovery are best shown by the corresponding weighted impact pressure coefficient (fig. 7). At an angle of attack of 0° , there were only small variations in inlet impact pressure coefficient above an inlet-velocity ratio of 0.45 and losses between the inlet and diffuser varied from $0.02(H_0 - p_0)$ to $0.03(H_0 - p_0)$ for the range shown. Below 0.45, where separation losses became severe, the pressure coefficient dropped off rapidly.

The inlet and diffuser impact pressure coefficients in the low inlet-velocity-ratio range improved with increasing angle of attack because of the aforementioned flow spillage from the top of the inlet and to a slight thinning of the spinner boundary layer in the lower regions. The actual values of the coefficients in the range of low inlet-velocity ratio were difficult to determine since it is not possible to evaluate accurately the regions where reversed flow is indicated at the inlet (zero flow was assumed for integration purposes) and the exact extent of flow asymmetry at both rake stations may not have been determined with the present instrumentation. Evaluation of the impact pressures obtained at the venturi, where the duct was more completely instrumented and the flow was symmetrical, however, showed that these increases between 0° and 5° were of the right order. In addition, measurements of the mass flow at the two stations showed excellent agreement. As already pointed out, figure 7 indicates that, at the test angles of attack, the diffuser pressure coefficients

decreased with an increase in flow rate as flow began entering the top portion of the inlet and then became higher with a further increase in flow rate when separation from the top of the spinner was eliminated. The increases in impact pressure with angle of attack at low values of the inlet-velocity ratio are obviously associated with higher external drag. A more important adverse effect, however, might be the influence of the flow asymmetry on the loading of the compressor blades of a gas-turbine-engine installation.

The effect of Mach number on the average impact pressure coefficients at the inlet and diffuser is presented in figure 8. No appreciable differences were found in the pressures above the knee of the curves over the range of test Mach number. Below this point, however, the variations were sometimes large. The reasons for the spread are not readily apparent, but are believed to be of secondary importance since these variations occur below an operational inlet-velocity ratio.

Basic configuration, propeller installed.- Representative total- and static-pressure distributions at inlet and diffuser measuring stations with the sealed juncture propeller operating at the design cruise condition are shown in figure 9 for $M_0 = 0.68$ at angles of attack of 0° and 5° . In general, the local impact pressure coefficients never attained the propeller-removed values at $\alpha = 0^\circ$, except in the outer region of the inlet annulus, because of the shank and shank-spinner-juncture interference effects on the spinner boundary layer (compare with fig. 6). These effects might have been expected to cause separation at higher inlet-velocity ratios than with propeller removed. Such separation did not occur; this result is similar to that obtained in reference 2. Propeller operation also stabilized the entering flow and asymmetry of the total-pressure distribution was not present at 0° angle of attack. The main effect of propeller operation at angle of attack was to eliminate a portion of the reversal of flow and the surge which occurred with propeller removed at the low inlet-velocity ratios.

Average impact pressure coefficients at the inlet and diffuser with propeller operating at the design cruise condition are presented in figure 10 as a function of inlet-velocity ratio for the test angles of attack at $M_0 = 0.68$. At $\alpha = 0^\circ$, the coefficients at the inlet were from 0.01 to 0.06 less than with propeller removed (compare with fig. 7) over the range of inlet-velocity ratio. The greater inlet losses occurred at and below the knee values of inlet-velocity ratio, where the shank interference effects on the spinner boundary layer were greatest; the knee of these curves indicates the inlet-velocity ratio below which losses due to separation increase in severity. Losses in pressure between the inlet and diffuser were about equal for propeller removed and with propeller operating at inlet-velocity ratios below the knee values. For inlet-velocity ratios above the knee values, however, the losses with propeller operating were about twice those

with propeller removed (from about $0.05(H_0 - p_0)$ to $0.07(H_0 - p_0)$), probably because of additional mixing and growth of the thickened inlet boundary layer inside the diffuser section. It should be noted that retwisting the shank sections of the present propeller would not effect significant increases in recovery. For a lower advance ratio design, however, possible increases in recovery might be obtained by increasing the thrust loading of the shank sections.

At the lower inlet-velocity ratios for the 2.5° and 5° angle-of-attack cases, the average impact pressure coefficient decreased with increasing flow rate. This initial reduction was effected by the entry of low energy air in the upper portions of the inlet where reversed flow was indicated for the propeller-removed case. The diffuser pressure coefficients, however, followed the same trend as that obtained with propeller removed. For inlet-velocity ratios below 0.4, some points on these curves indicated slightly higher pressures at the diffuser than at the inlet. This apparent anomaly is due to the influence of asymmetrical flow on the measurements made with the present instrumentation.

The inlet impact pressure coefficient obtained with the sealed shank propeller operating over the test range of Mach number, advance ratio, and blade angle is presented in figure 11 for an angle of attack of 0° ; corresponding results of propeller-removed case are included for comparison. Only a slight effect of Mach number is noted with the propeller operating at the design cruise condition ($\beta_F = 63.1^\circ$; $\beta_R = 62.3^\circ$; $V/nD = 4.2$). A reduction in advance ratio to 3.5, with resultant higher root angles of attack, caused small increases in the pressure coefficients as might be anticipated from low-speed data (ref. 2). The increased root angles of attack, however, might also be expected to cause additional shock and shock-boundary-layer effects at the higher Mach numbers, and the data for an advance ratio of 3.5 indicate a tendency toward an increased compressibility effect. At the simulated high-speed condition ($\beta_F = 67.4^\circ$; $\beta_R = 66.6^\circ$; $V/nD = 5.25$), the Mach number effect became more pronounced and the pressure coefficients did not increase with increases in shank loading as the advance ratio was reduced from 5.25 to 4.2. It is apparent that thinner shank sections will be required to obtain any significant increases in impact pressures. This conclusion is in agreement with the data of references 6 and 7, in which the section characteristics of several two-dimensional 16-series airfoils, with varying thickness ratios are reported. Reference 6 indicates that, for airfoil sections in the range of thickness of the present shanks, the lift is markedly reduced and the drag increased by increases in thickness ratio. Reference 7 further points out that the only practical method of reducing compressibility losses is by decreasing the section thickness ratio.

With the platform-type juncture installed, only a slight effect of Mach number on the inlet impact pressure (fig. 12) was noted for the entire test range of advance ratio and blade angles. The reduction in the adverse compressibility effects for the platform-juncture configuration as compared with the sealed shank propeller is probably due to the following factors: At the cruise blade angle, where the propeller shanks and the platform juncture were aligned, some relief of the pressures on the suction face of the blades may be afforded by the gap. For the high-speed condition, where the compressibility effects for the sealed shank configuration were most pronounced, in addition to the gap effects, the angles of attack of the fixed platform sections were less than those for the comparable shanks of the sealed juncture configuration inasmuch as the platforms remained fixed at the cruise attitude. The possible generation of vortices at the juncture gap (see ref. 8) may also have been influential at the high-speed blade angle.

Average impact pressure coefficients obtained with the two propeller shank-spinner juncture configurations are compared in figure 13 at the design Mach number. Although the effects of compressibility on the impact pressures were smaller for the platform juncture (compare figs. 11 and 12), the coefficients were generally reduced as compared to the sealed juncture propeller (fig. 13) in the operational range of inlet-velocity ratio.

For the design cruise blade angle, the impact pressure coefficients above the knee of the curves were about 4 percent of the stream impact pressure less than those for the sealed juncture propeller; the reduction in coefficients, of course, was a result of the flow through the gap. Similar losses were also obtained at the high-speed blade angle for Mach number below 0.79. For this condition, the decrease in pressure coefficients was apparently due to the reduced blade angle in the region of the fixed platform as well as to the gap flow. At $M_0 = 0.79$, the coefficients obtained with the two configurations were in better agreement (see fig. 13) because of the adverse effects of compressibility on the sealed juncture configuration.

For the previous low-speed investigation (ref. 2), a juncture gap one-half as large as the present one was considered and the impact pressure coefficients for the sealed and the platform junctures compared more favorably over the entire test range. It has been determined, however, that the former gap was not a practical one (ref. 9) and it was increased, therefore, for the present test. Because of the effects of gap size on the pressure coefficients, it is indicated that some type of seal that would not cause disturbances to the entering flow would be advantageous. This fact is most obvious at the cruise blade angle where the advantages of the gap flow, from the standpoint of decreased compressibility effects, are small compared to the pressure losses. At the high-speed blade angle, where the compressibility effects

for the sealed juncture became greater ($M_0 = 0.79$) and some relief is afforded by the platform-juncture configuration, the over-all influence of a gap seal is not so apparent.

Effect of variations in inlet height and internal diffusion.-

Representative distributions of total- and static-pressure coefficients measured at one of the inlet rakes of each of the four cowlings with the NACA 1-51.6-094.4 spinner are presented in figure 14 for an angle of attack of 0° at a Mach number of 0.3. These distributions and those at the other rake stations (not shown) indicate that the boundary-layer thickness at comparable inlet-velocity ratios was similar for all configurations until separation occurred ahead of the inlet. These effects are also shown in figure 15 where the boundary-layer thickness, defined as the normal distance from the surface to the point where

$\frac{H_1 - p_0}{H_0 - p_0} = 0.95$, is presented as a function of inlet-velocity ratio.

The "knees" at the lower values of inlet-velocity ratio where the thickness began to increase rapidly are indicative of the onset of separation. It is apparent from these data that the separation value of inlet-velocity was not significantly affected by variation in inlet height for heights as low as $0.055D_c$ or rate of internal compression. The representative boundary-layer thicknesses shown for each configuration were within ± 0.03 inch of the values measured at all inlet rakes for inlet-velocity ratios above 0.39. Below this point, the flow asymmetry became severe and surging was noted around the annulus.

The inlet and diffuser average impact pressure coefficient for the four cowling configurations is shown in figure 16 as a function of inlet-velocity ratio for angles of attack of 0° , 2.5° , and 5° . As would be expected, the inlet coefficients improved with increasing inlet height inasmuch as the boundary layer, which is similar for all cases, filled a smaller part of the total area. This fact is especially true in the diffuser where the boundary layers from the inner- and outerduct walls were in closer proximity for the smaller inlet and greater mixing of the two boundary regions occurred.

The results obtained with the NACA 1-69.8-077.7 cowling with and without a diffuser, indicates that there is a negligible difference in inlet impact pressure recovery for the entire range of inlet-velocity ratio. At the diffuser station, however, the internal pressure rise at low inlet-velocity ratios effected internal separation for the diffuser configuration; greater total-pressure losses resulted from this separation. When internal separation was eliminated ($V_1/V_0 \approx 0.50$ for $\alpha = 0^\circ$), the recovery for this configuration equaled or was higher than the case with no internal compression due to reduced skin-friction losses. An inlet-velocity ratio greater than this value is required to avoid a pressure peak on the lip of any NACA 1-series cowling usable

with this spinner and designed for a critical Mach number of 0.80 and above (see fig. 99 of ref. 1).

The angle-of-attack effects were similar to those previously discussed in connection with the basic configuration with propeller removed. At the low inlet-velocity ratios, the diffuser recovery was often higher than that at the inlet for 2.5° and 5° . As previously pointed out, this is apparently due to the effects of flow asymmetry on the measurements made with the present instrumentation.

CONCLUDING REMARKS

An investigation has been conducted to study the effects of compressibility at Mach numbers up to 0.8 on the internal-flow characteristics of an NACA 1-series cowling-spinner combination equipped with a dual-rotation propeller. Two 24-percent-thick shank propellers were studied; one had a sealed propeller-spinner juncture and the other had a raised-platform airfoil-shaped juncture. The effects of inlet height and rate of internal compression, with propeller removed, was also considered. The more important conclusions are as follows:

1. The effects of compressibility on the basic configuration with propeller removed are negligible for the entire test range.
2. The propeller caused no appreciable compressibility effects on the internal impact-pressure when operating at the design cruise condition. With increases in shank loading, however, shock and shock-boundary layer interaction effects caused reductions in impact pressure at a Mach number of 0.8 for the sealed shank propeller.
3. Installation of the platform-type propeller-spinner juncture configuration investigated with a blade-platform gap height of 0.02 inch (approx. $1/8$ inch full scale) caused a reduction in inlet impact pressure coefficient of about 4 percent for the propeller design cruise blade angle.
4. Inlet height (as low as $0.055D_c$ where D_c is maximum diameter of cowling) and rate of internal compression had no significant effect on the inlet-velocity ratio at which separation from the spinner occurred.

Langley Aeronautical Laboratory,
National Advisory Committee for Aeronautics,
Langley Field, Va.

REFERENCES

1. Nichols, Mark R. and Keith, Arvid L., Jr.: Investigation of a Systematic Group of NACA 1-Series Cowlings With and Without Spinners. NACA Rep. 950, 1949. (Supersedes NACA RM L8A15.)
2. Keith, Arvid L., Jr., Bingham, Gene J., and Rubin, Arnold J.: Effects of Propeller-Shank Geometry and Propeller-Spinner-Juncture Configuration on Characteristics of an NACA 1-Series Cowling-Spinner Combination With an Eight-Blade Dual-Rotation Propeller. NACA RM L51F26, 1951.
3. Sammonds, Robert I., and Molk, Ashley J.: Effects of Propeller-Spinner Juncture on the Pressure-Recovery Characteristics of an NACA 1-Series D-Type Cowl in Combination With a Four-Blade Single-Rotation Propeller at Mach Numbers up to 0.83 and at an Angle of Attack of 0°. NACA RM A52D01a, 1952.
4. Gilman, Jean, Jr., Crigler, John L., and McLean, F. Edward: Analytical Investigation of Propeller Efficiency at High-Subsonic Flight Speeds Near Mach Number Unity. NACA RM L9L05a, 1950.
5. Von Doenhoff, Albert E., and Braslow, Albert L.: Studies of the Use of Freon-12 As a Testing Medium in the Langley Low-Turbulence Pressure Tunnel. NACA RM L51L11, 1951.
6. Lindsey, W. F., Stevenson, D. B., and Daley, Bernard N.: Aerodynamic Characteristics of 24 NACA 16-Series Airfoils at Mach Numbers Between 0.3 and 0.8. NACA TN 1546, 1948.
7. Daley, Bernard N., and Humphreys, Milton D.: Effects of Compressibility on the Flow Past Thick Airfoil Sections. NACA TN 1657, 1948.
8. Taylor, H. D.: Summary Report on Vortex Generators. U.A.C. Rep. R-05280-9, United Aircraft Corp. Res. Dept., March 7, 1950.
9. Prince, Clifford H.: The Effects of Three Types of Propeller Shanks on Pressure Recovery of a Conical-Spinner-Turbine Intake at Mach Numbers of 0.4 and 0.7. U.A.C. Rep. R-14018-2, United Aircraft Corp. Res. Dept., June 29, 1948.

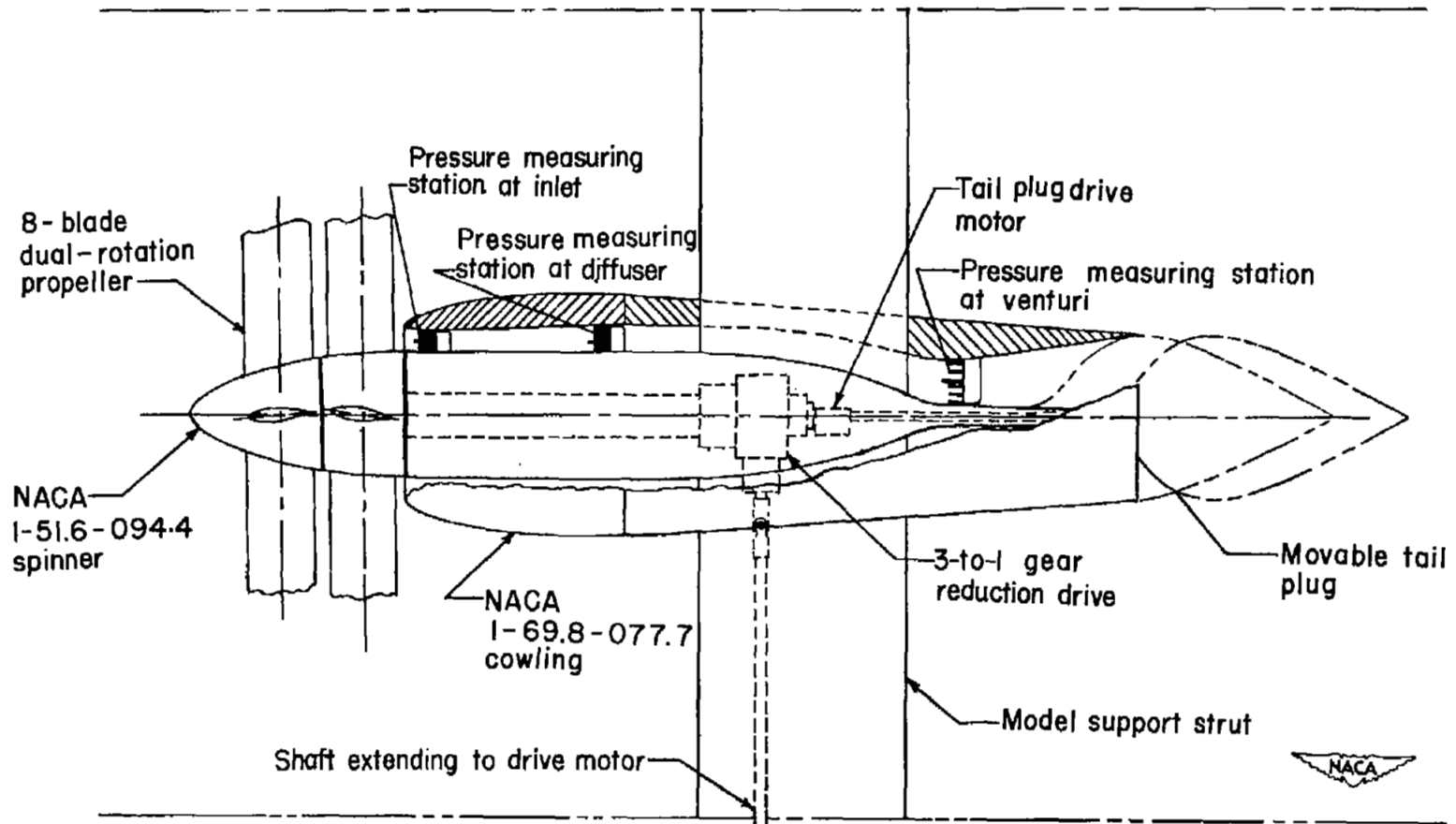
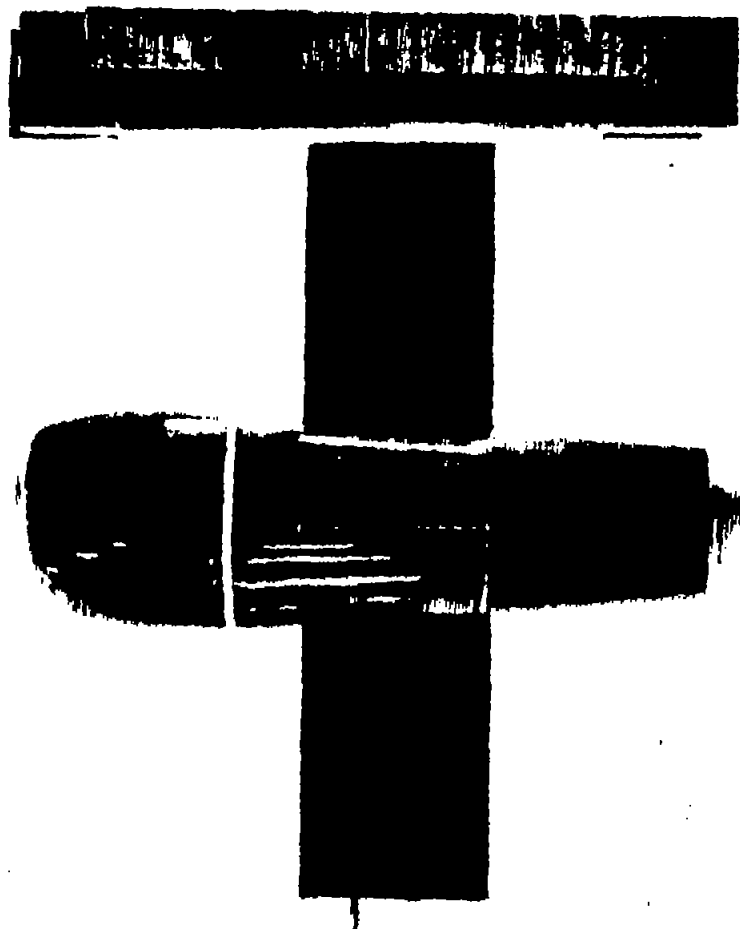


Figure 1.- General model arrangement. Plan view.

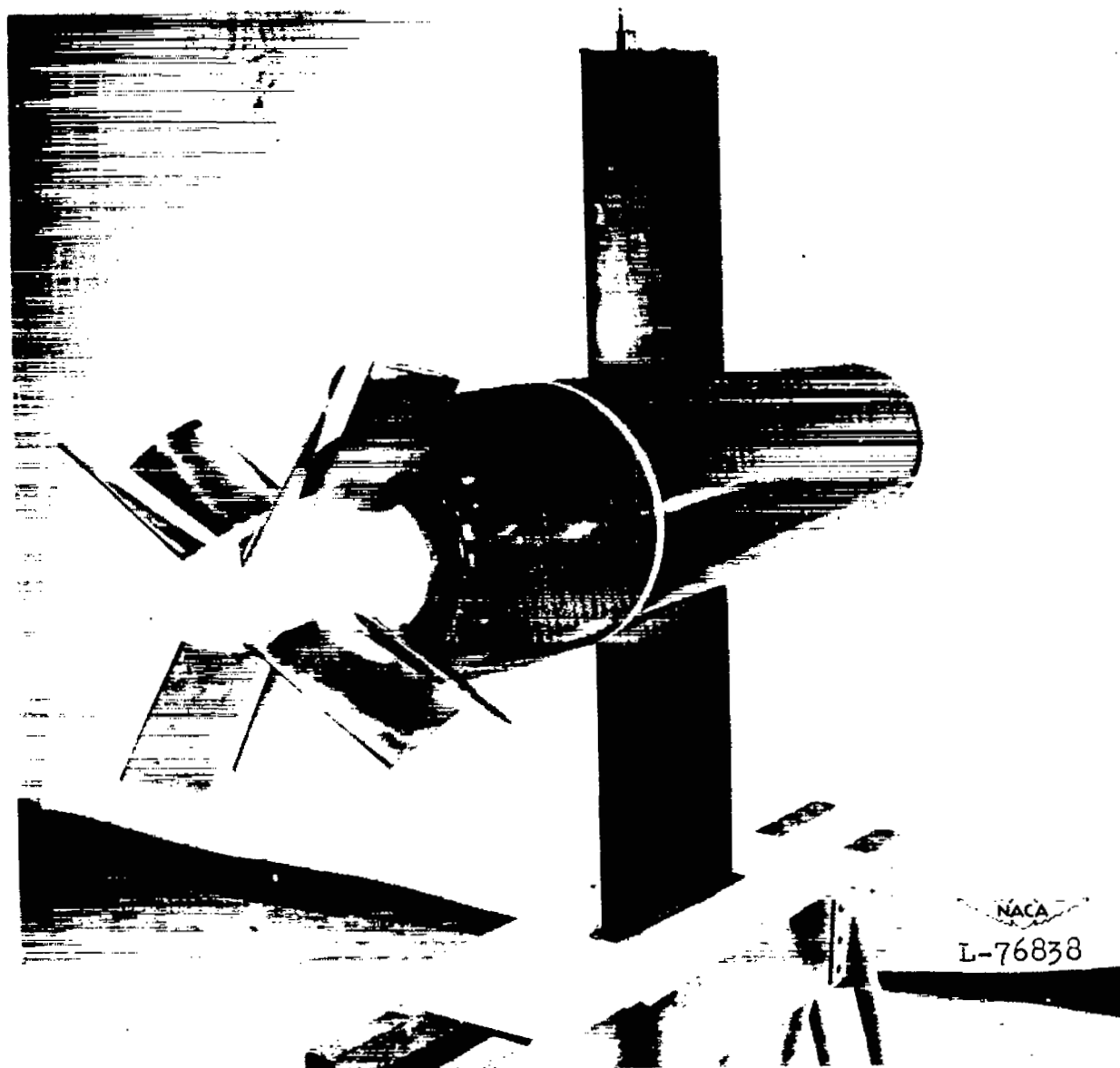


NACA

L-76835

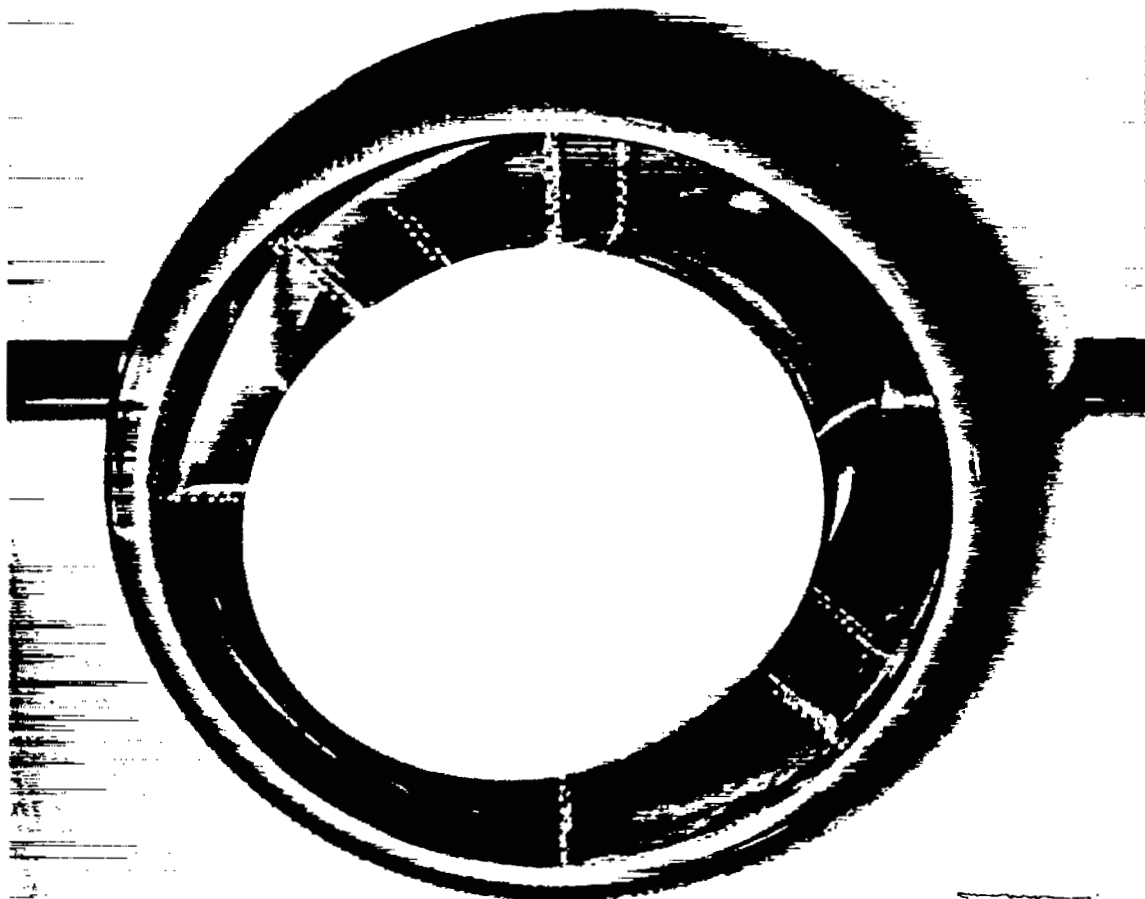
(a) Plan view of cowling-spinner combination. Propeller removed.

Figure 2.- Views of model.



(b) The 24-percent-thick shank propeller installed. Ideal juncture.

Figure 2.- Continued.



NACA
L-76837

(c) Front view of model showing tube arrangement.

Figure 2.- Concluded.

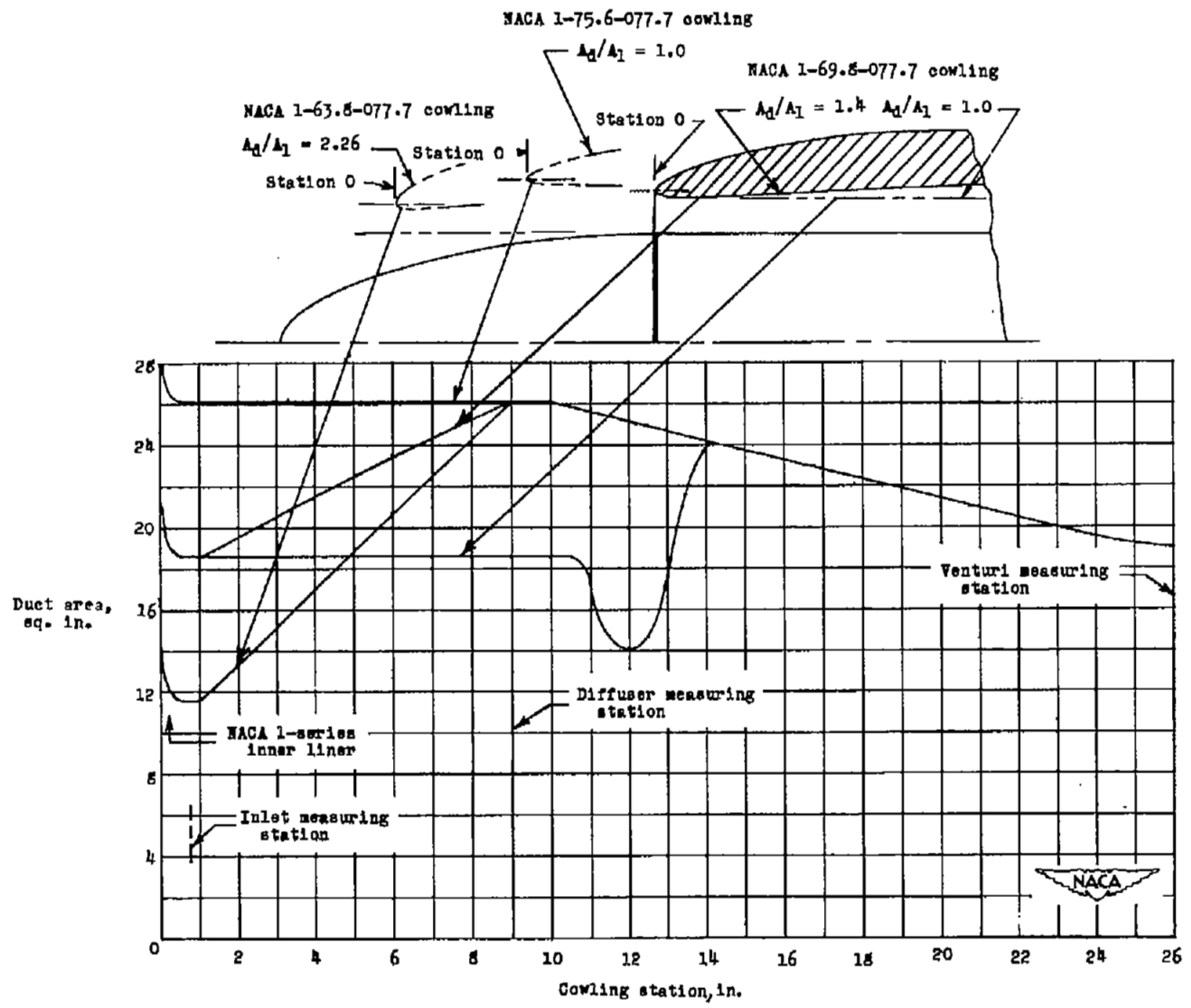


Figure 3.- Model area distribution.

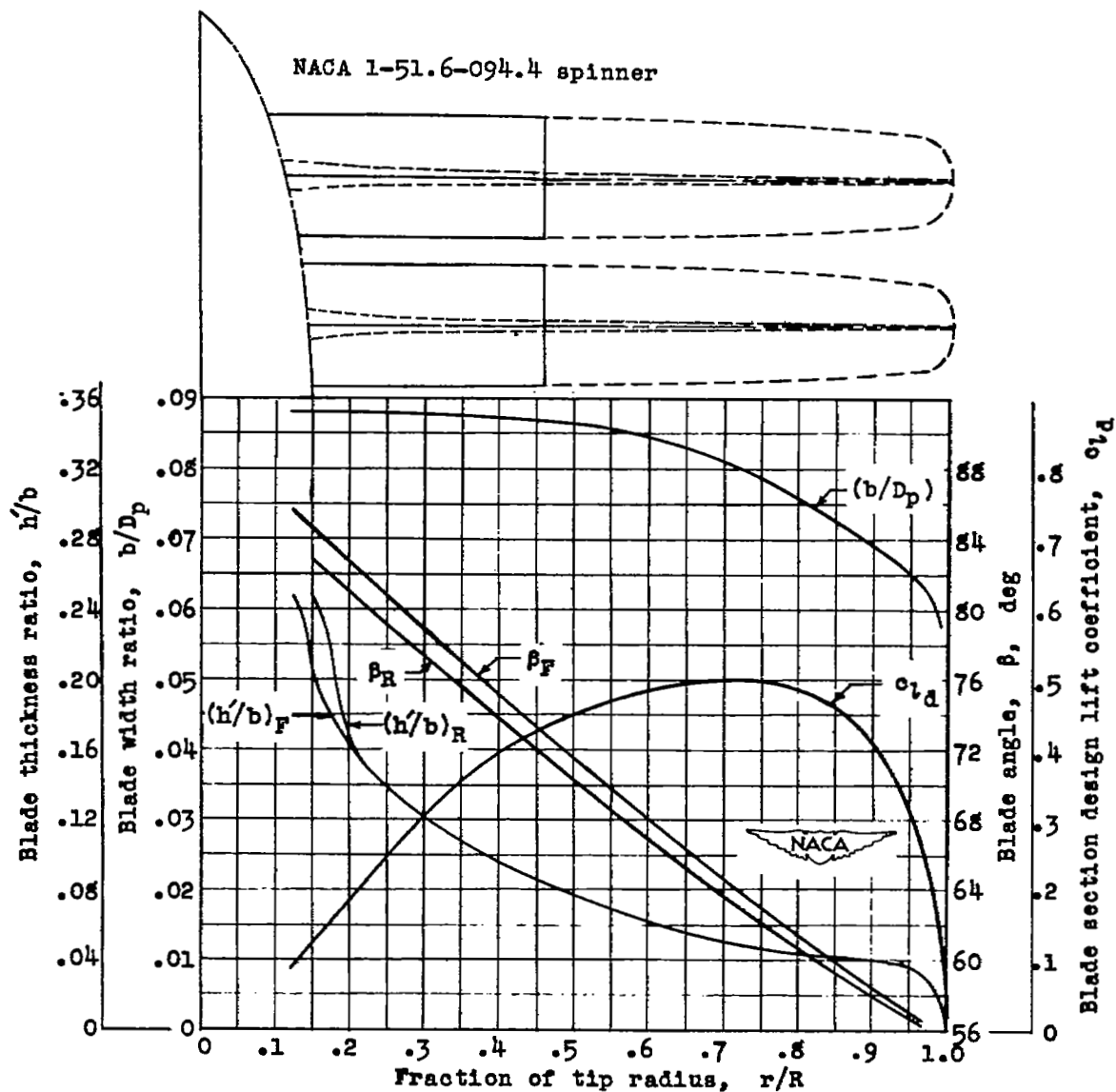
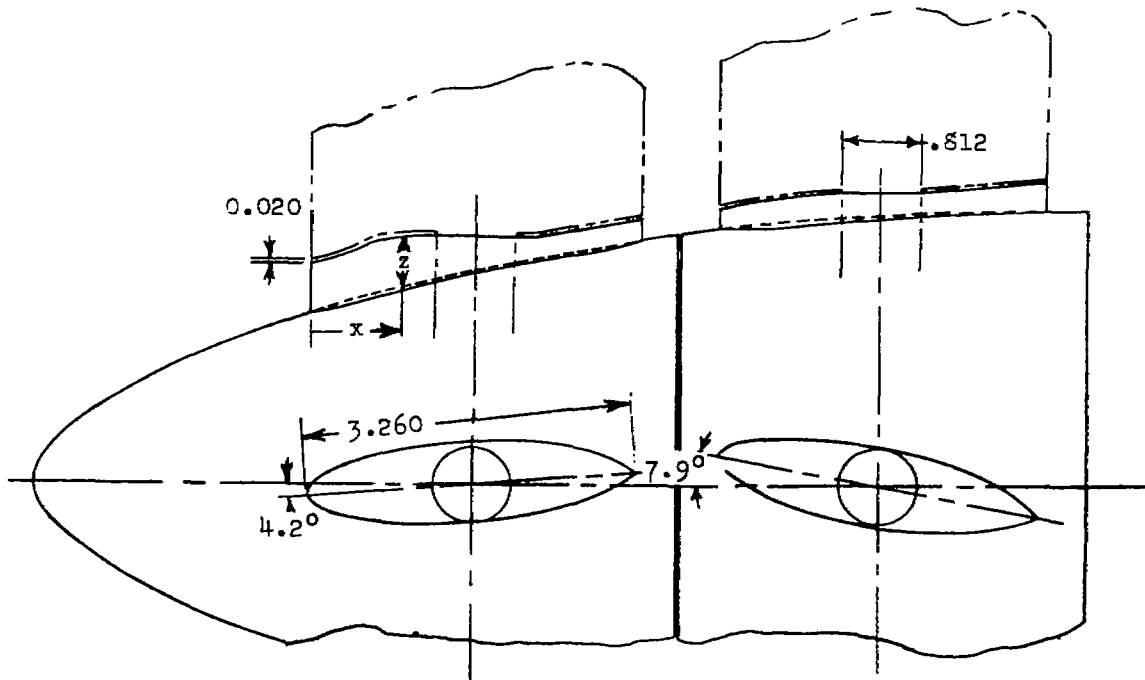


Figure 4.- Plan-form and blade-form curves for the 16-series, eight-blade, NACA 3.09-(5)(0.050)-04 dual-rotation propeller with 24-percent-thick shank sections. Test propeller cut off at $r/R = 0.459$.

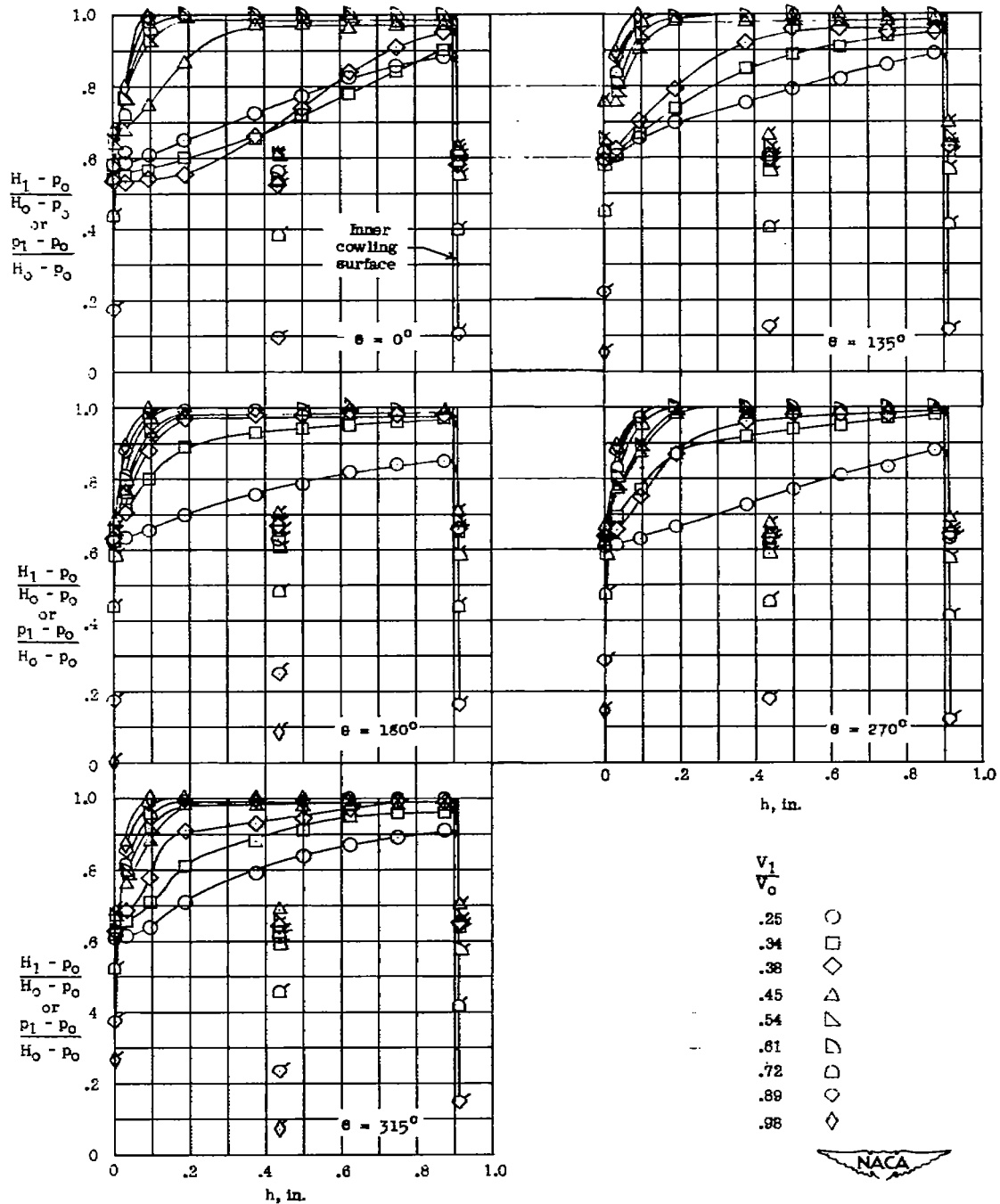


NACA

Front platform	
Station, x	Platform height, z
0	0.535
.375	.520
.625	.565
.750	.565
.875	.555
1.005	.530
2.245	.240
2.255	.245

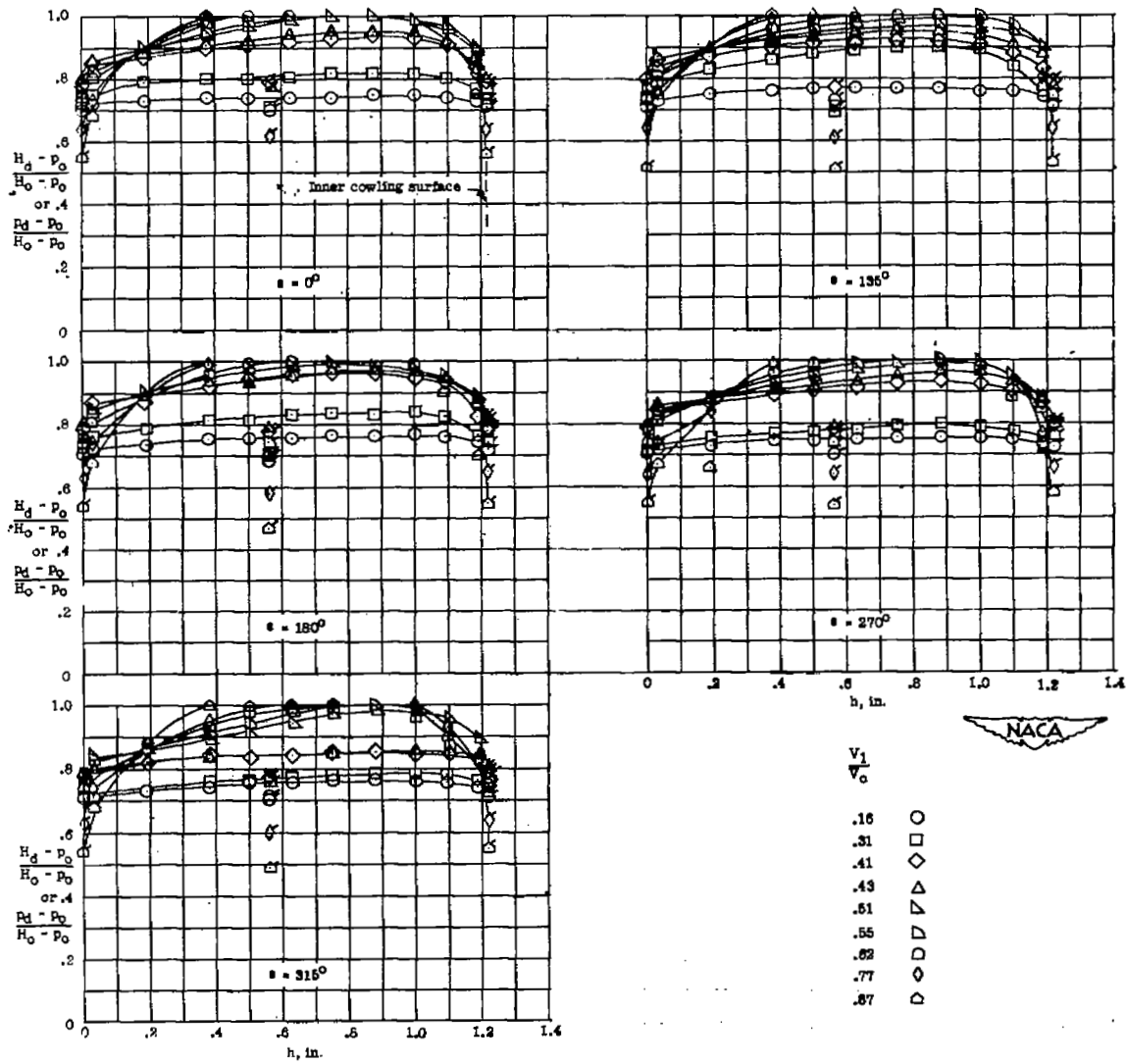
Rear platform	
Station, x	Platform height, z
0	0.265
.63	.299
1.38	.300
2.13	.252
2.88	.295
3.26	.335

Figure 5.- Platform-type juncture. Airfoil platform ordinates same as basic sealed juncture propeller. All dimensions are in inches.



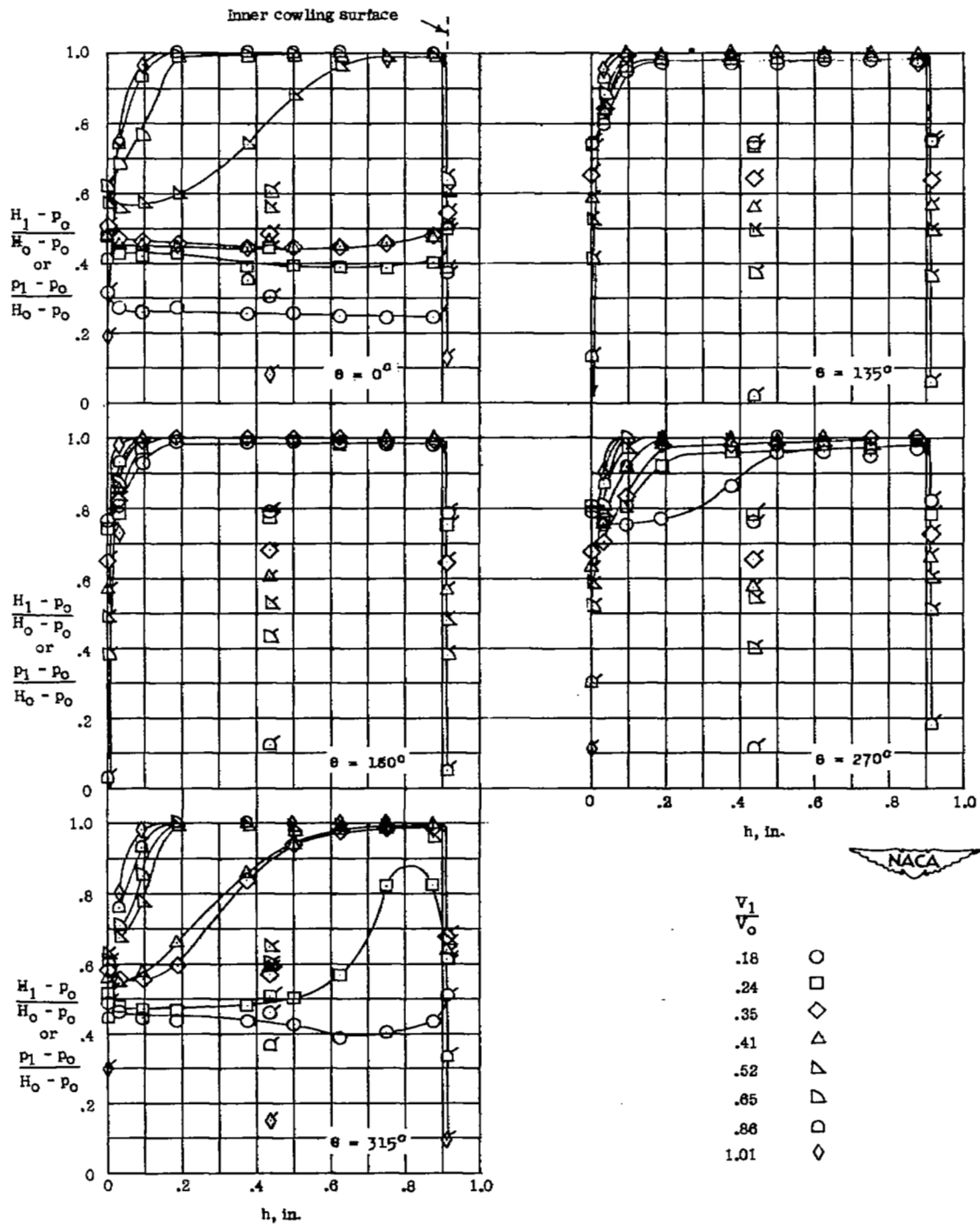
(a) Inlet. $\alpha = 0^\circ$.

Figure 6.- Total- and static-pressure distribution at inlet and diffuser measuring stations for basic cowling-spinner combination. Propeller removed; $M_0 = 0.68$. Flagged symbols indicate static pressures.



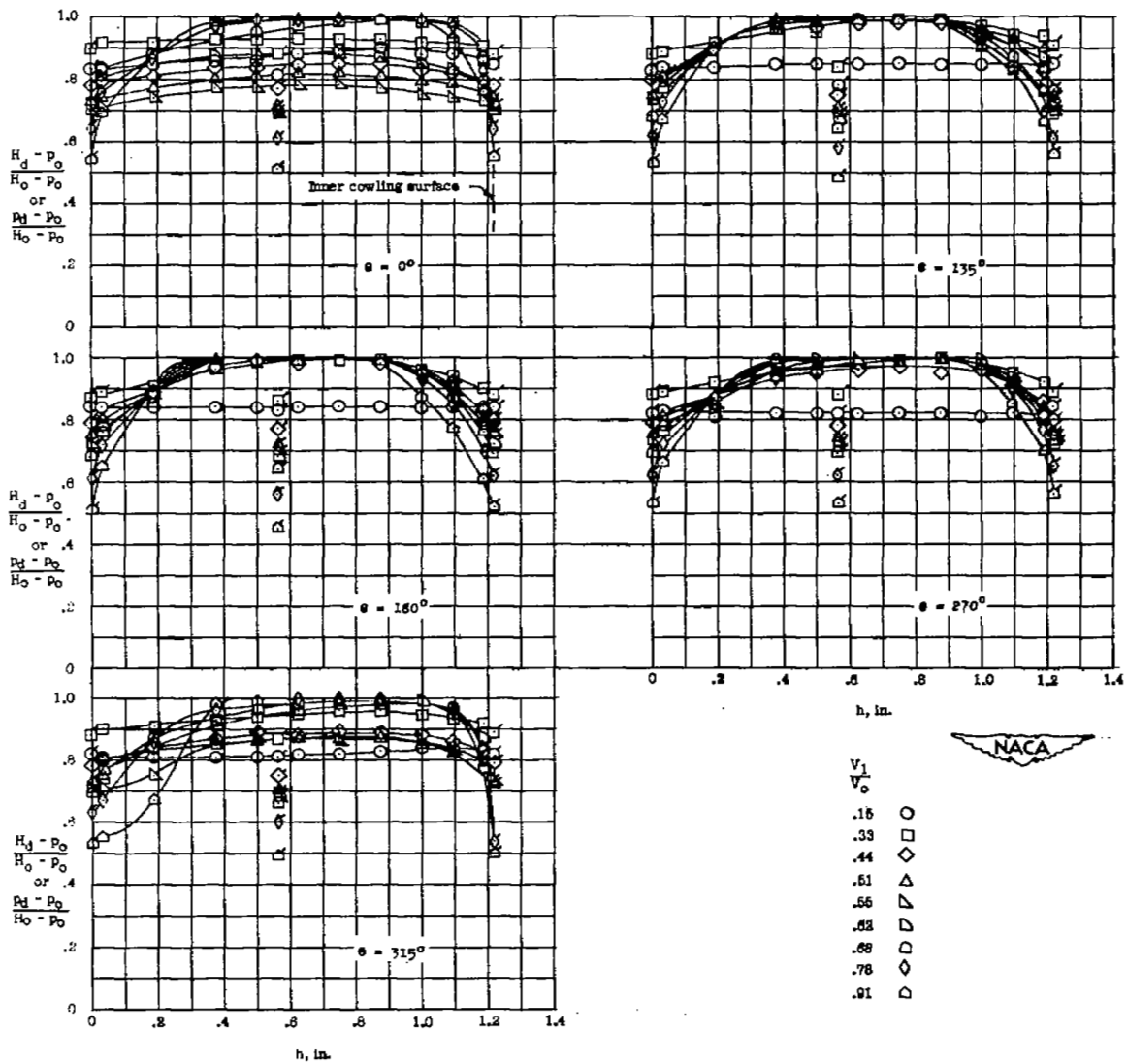
(b) Diffuser. $\alpha = 0^\circ$.

Figure 6.- Continued.



(c) Inlet. $\alpha = 5^\circ$.

Figure 6.- Continued.



(d) Diffuser. $\alpha = 5^\circ$.

Figure 6.- Concluded.

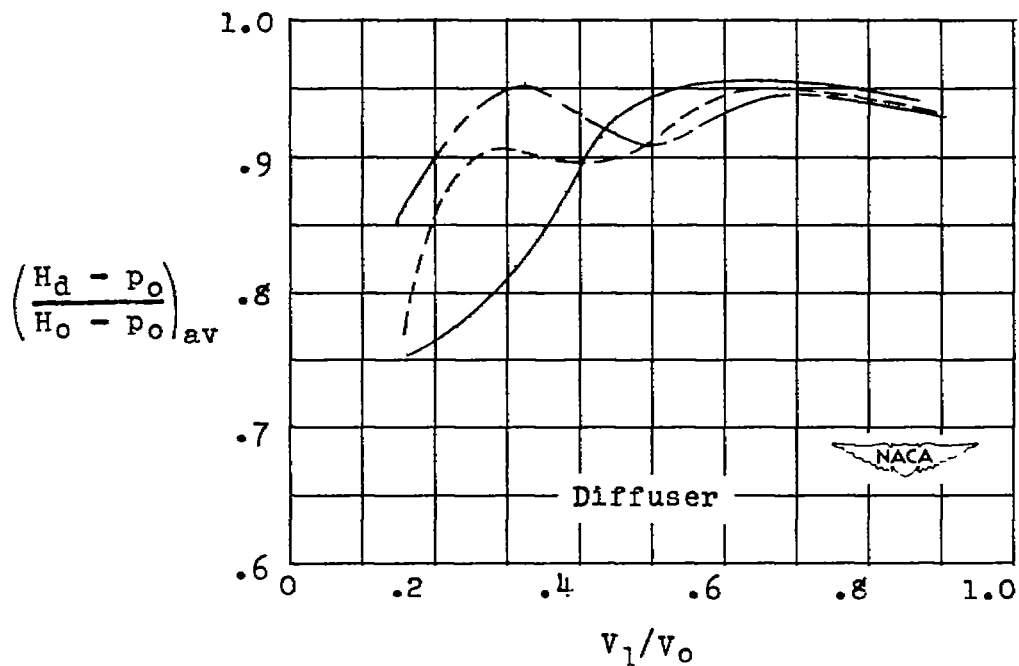
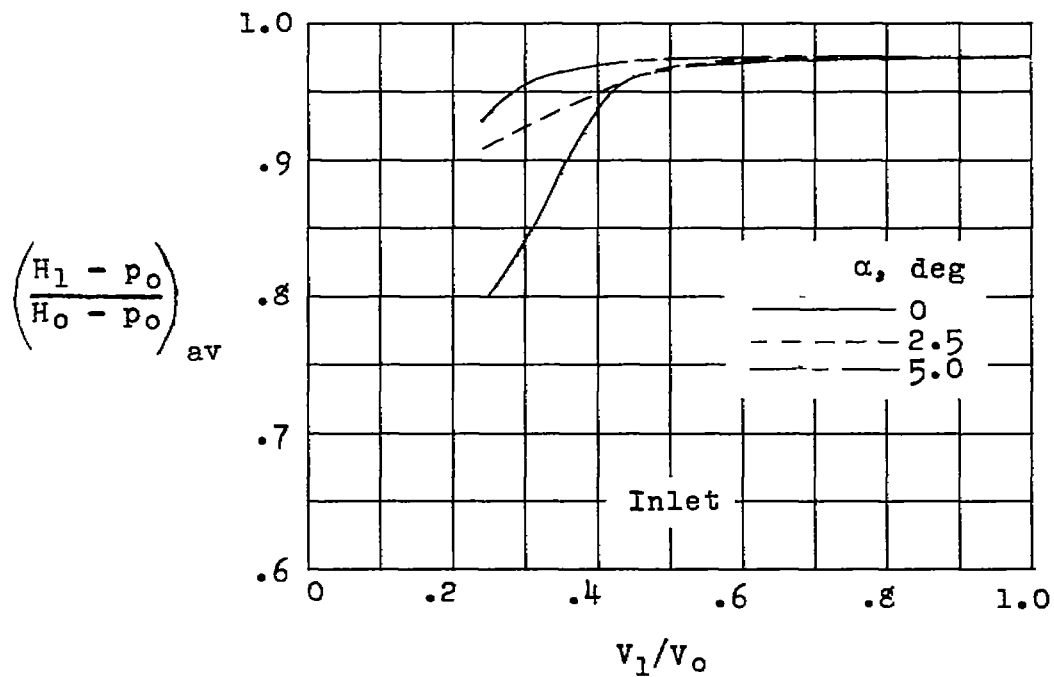


Figure 7.- Effect of inlet-velocity ratio and angle of attack on the average impact pressure coefficient at the inlet and diffuser. Propeller removed; $M_0 = 0.68$.

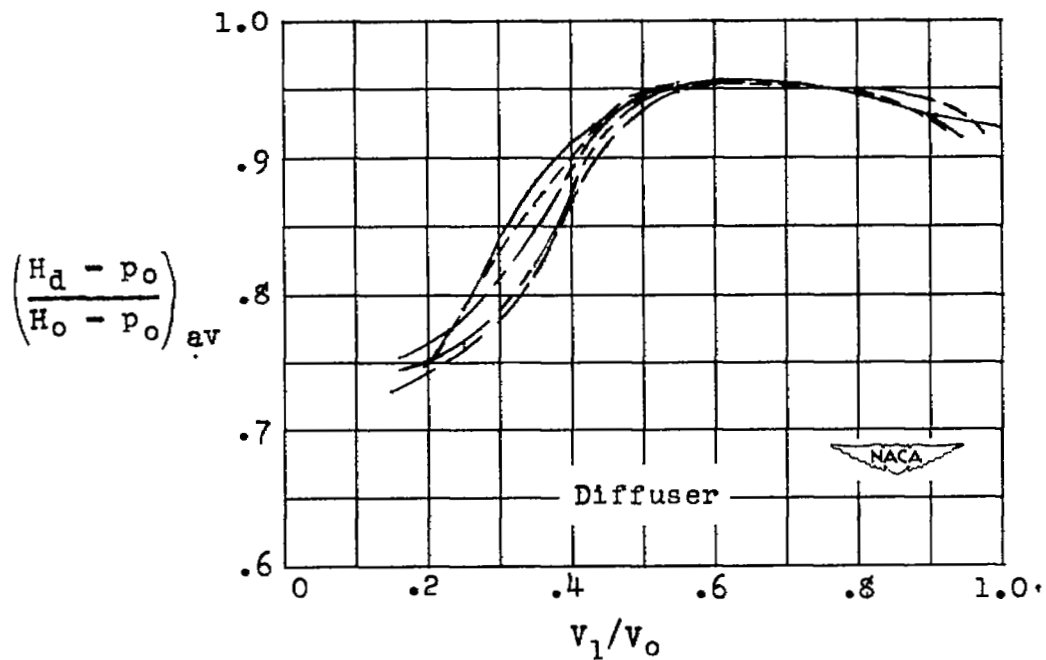
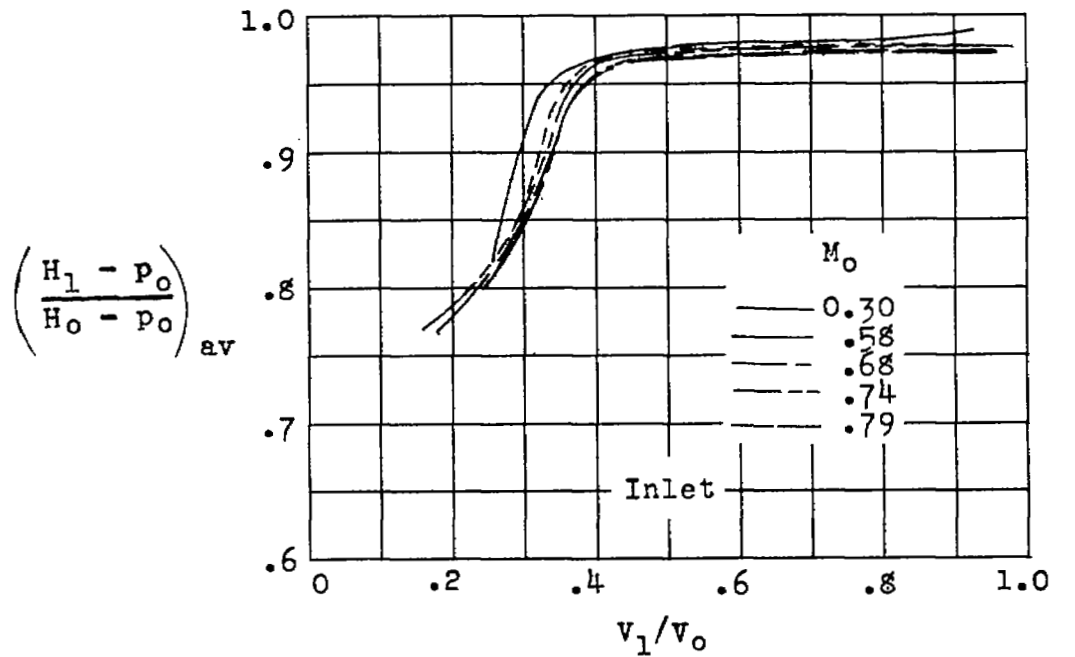
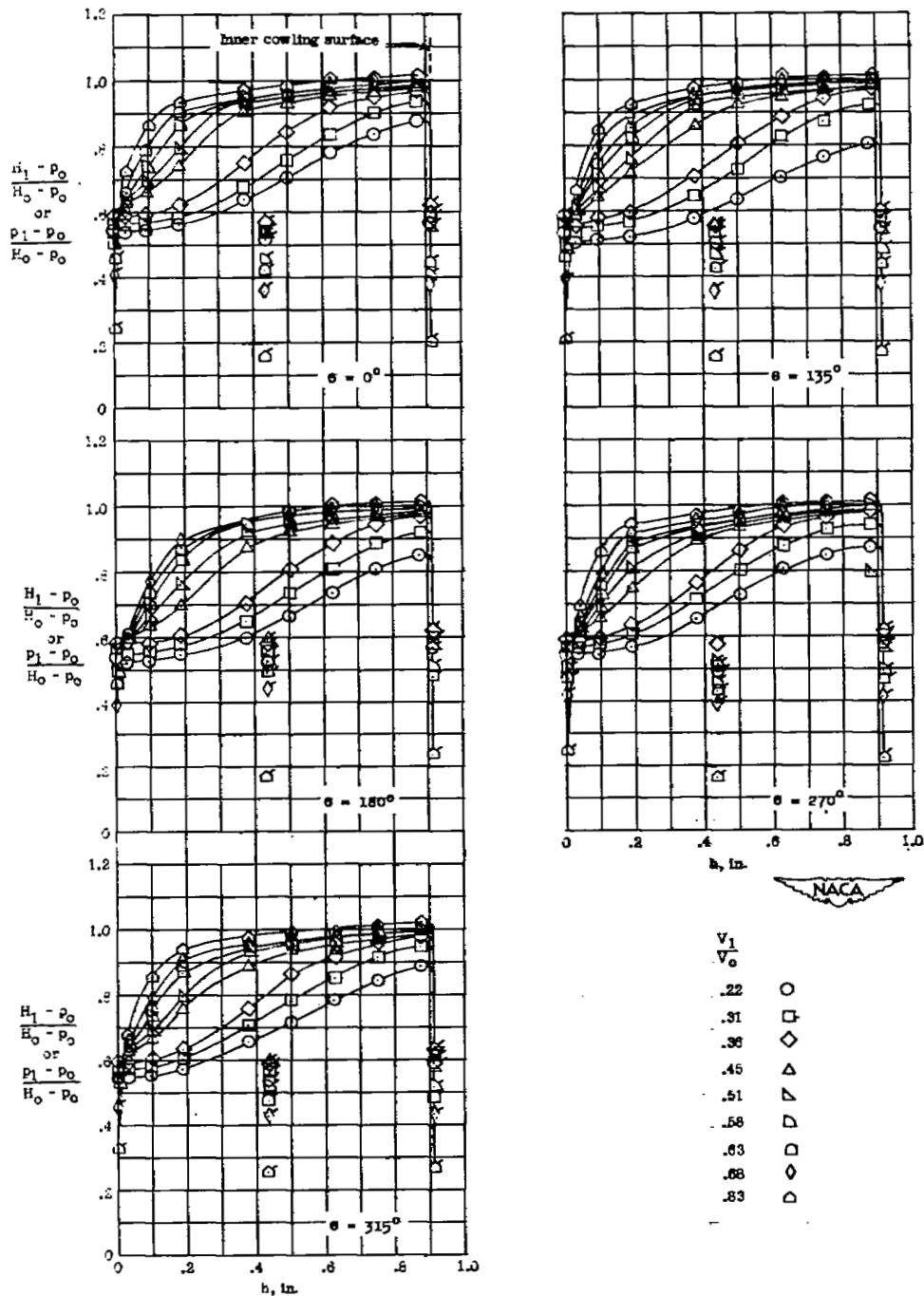
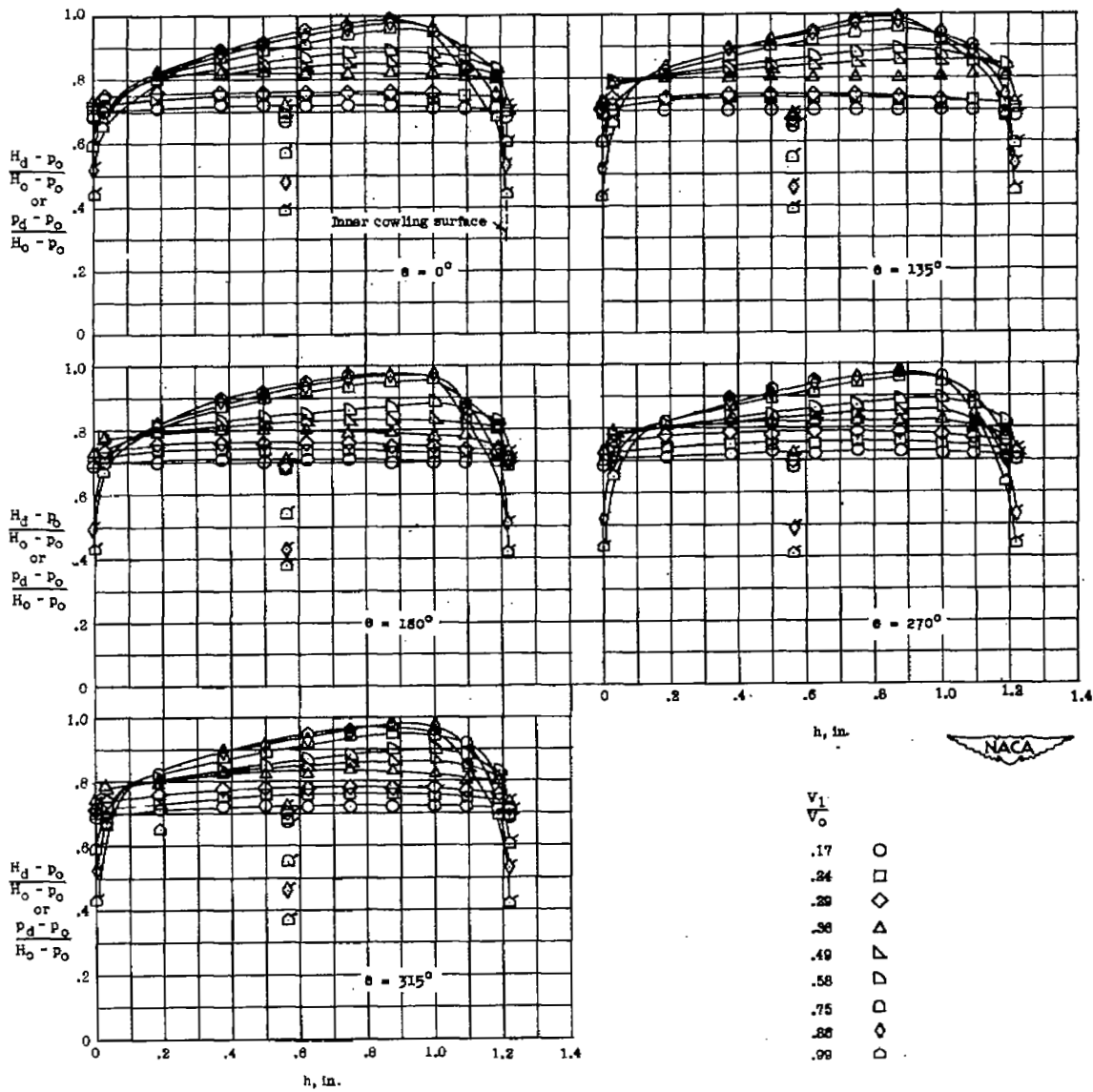


Figure 8.- Effect of Mach number on the average impact pressure coefficient at inlet and diffuser. Propeller removed; $\alpha = 0^\circ$.



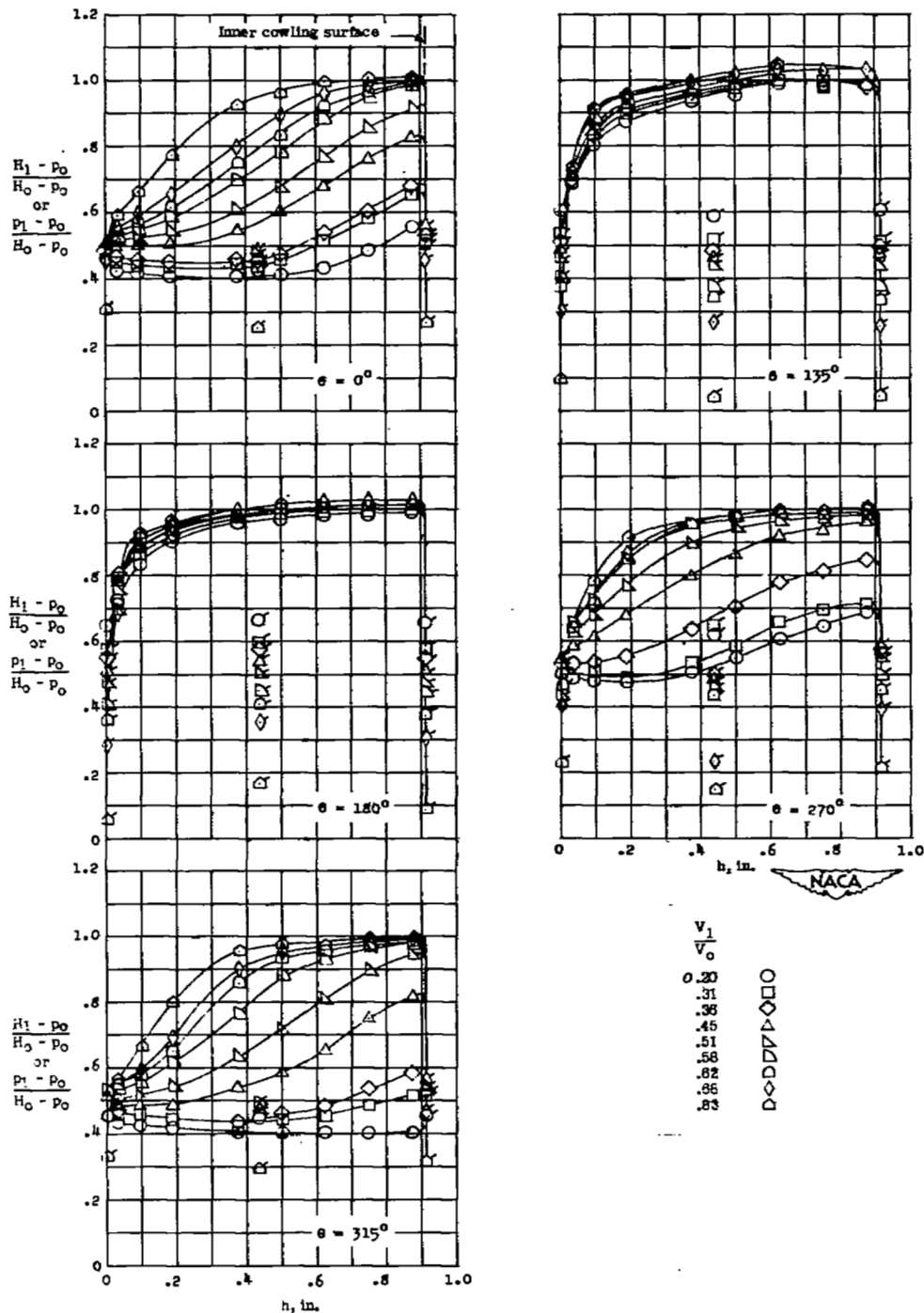
(a) Inlet. $\alpha = 0^\circ$.

Figure 9.- Total- and static-pressure distribution at inlet and diffuser measuring stations. Ideal shank-spinner juncture; $\beta_F = 63.1^\circ$; $\beta_R = 62.3^\circ$; $V/nD = 4.2$; $M_0 = 0.68$. Flagged symbols indicate static pressures.



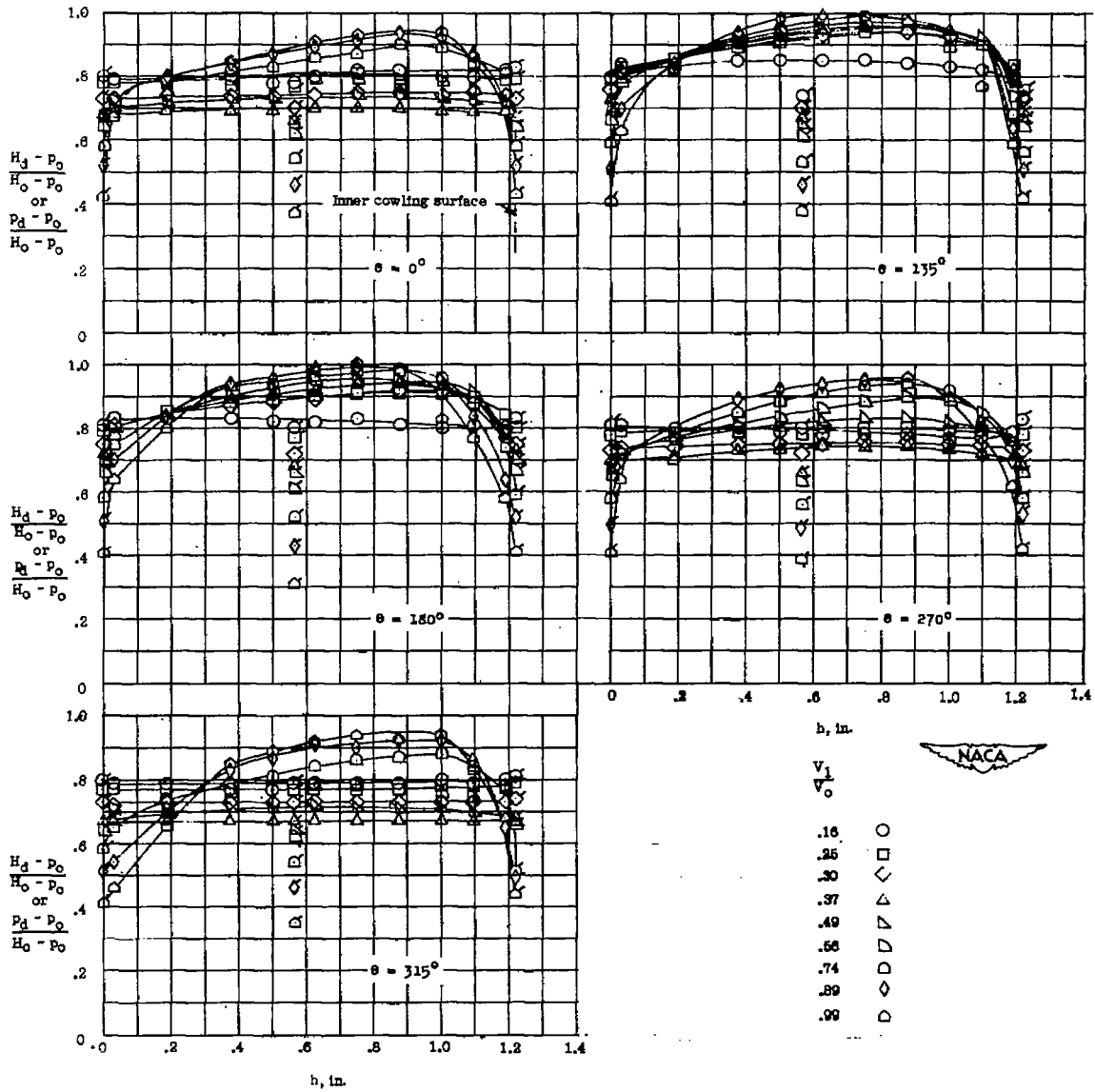
(b) Diffuser. $\alpha = 0^\circ$.

Figure 9.- Continued.



(c) Inlet. $\alpha = 5^\circ$.

Figure 9.- Continued.



(d) Diffuser. $\alpha = 5^\circ$.

Figure 9.- Concluded.

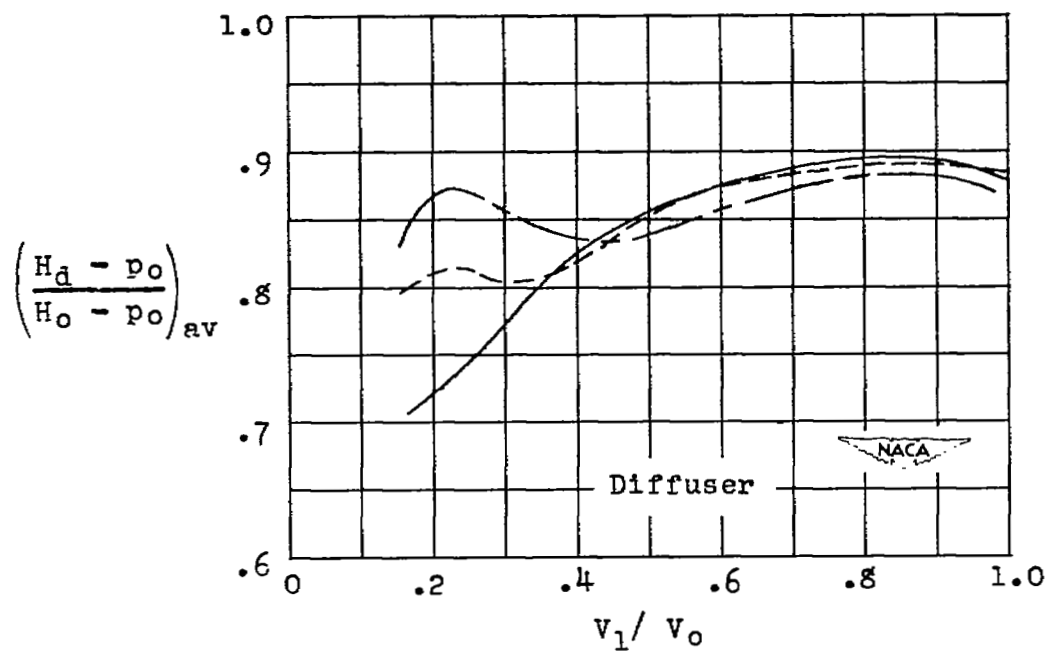
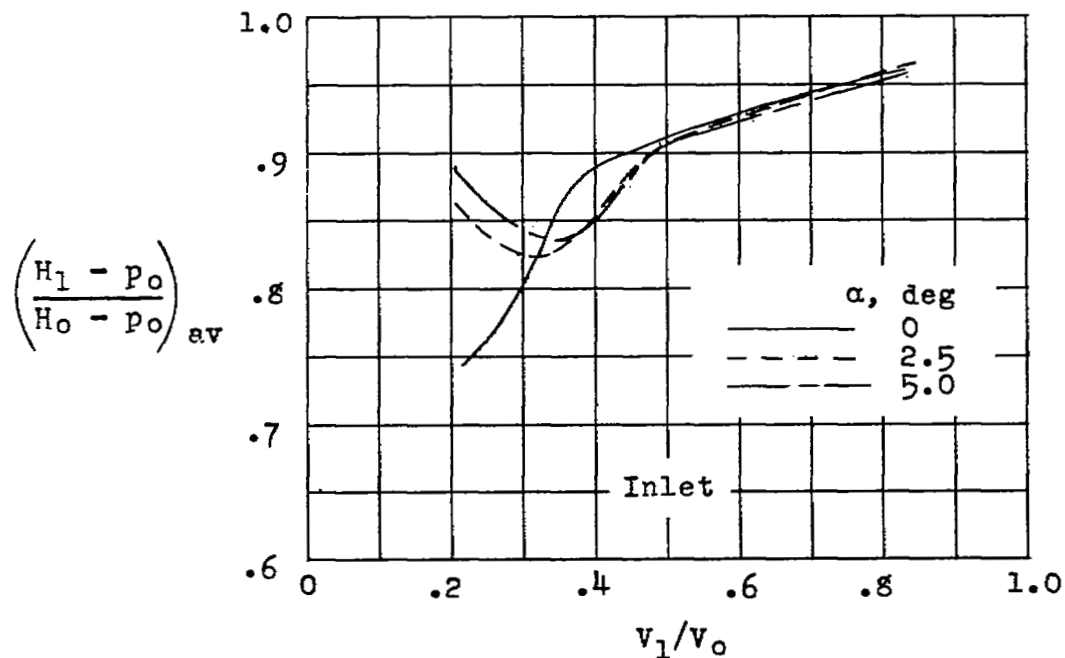


Figure 10.- Effect of inlet-velocity ratio and angle of attack on the average impact pressure coefficient at the inlet and diffuser. Ideal shank-spinner juncture; $\beta_F = 63.1^\circ$; $\beta_R = 62.3^\circ$; $V/nD = 4.2$; $M_o = 0.68$.

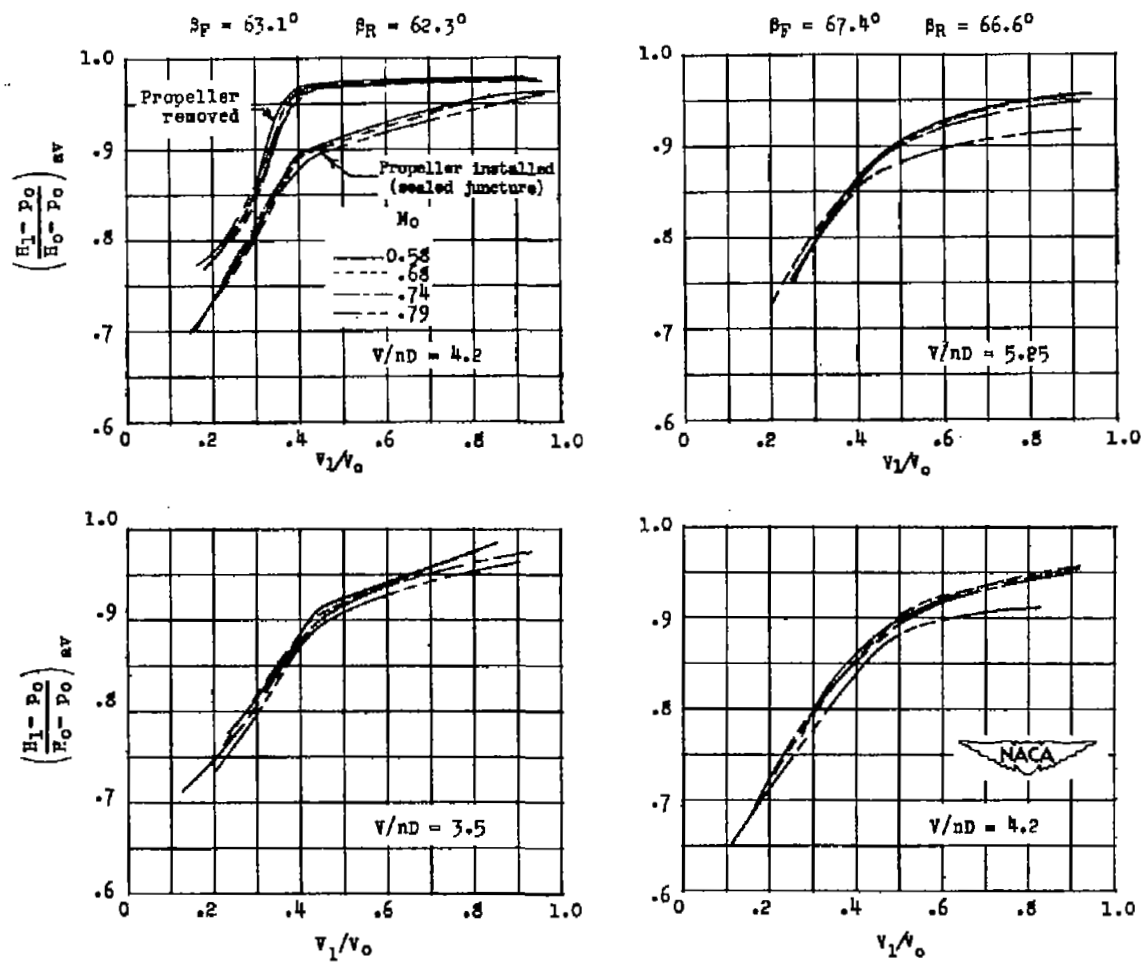


Figure 11.- Effect of Mach number on the average impact pressure coefficient at the inlet of the basic cowling with ideal shank-spinner-juncture propeller operating at the test blade angle and advance ratios. Propeller-removed data are included for comparison. $\alpha = 0^\circ$.

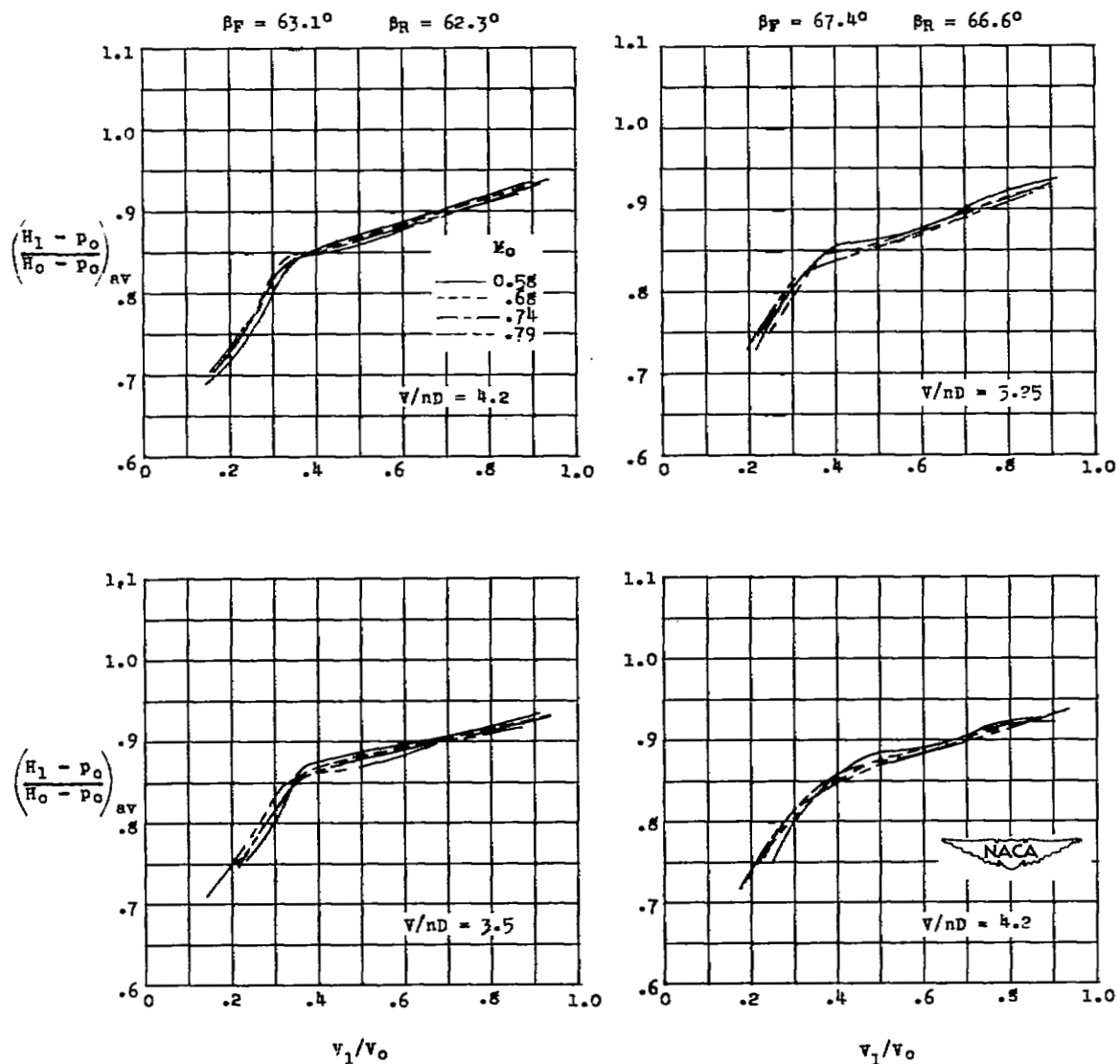


Figure 12.- Effect of Mach number on the average impact pressure coefficient at the inlet of the basic cowling with the platform-juncture propeller operating at the test blade angles and advance ratios. $\alpha = 0^\circ$.

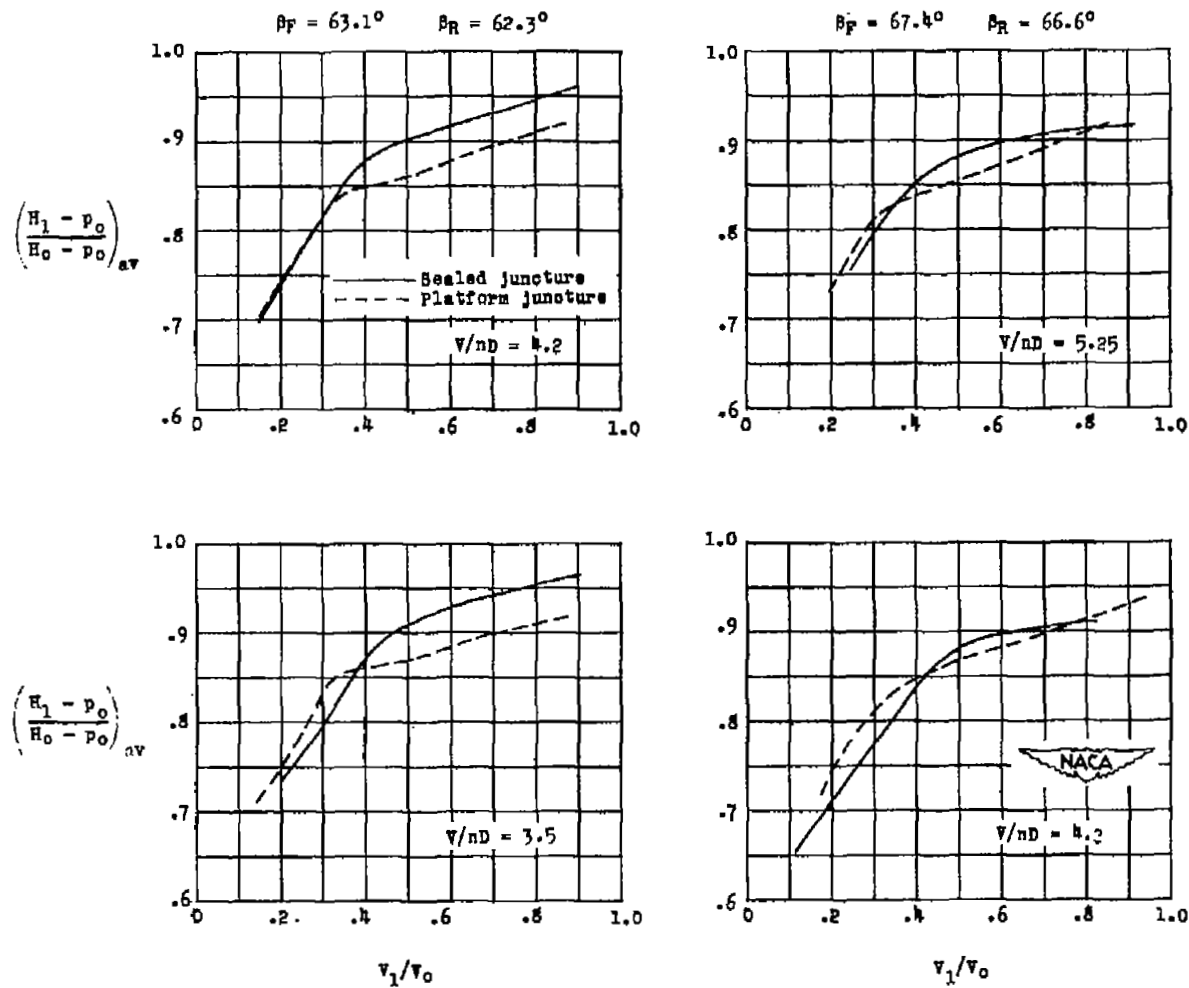
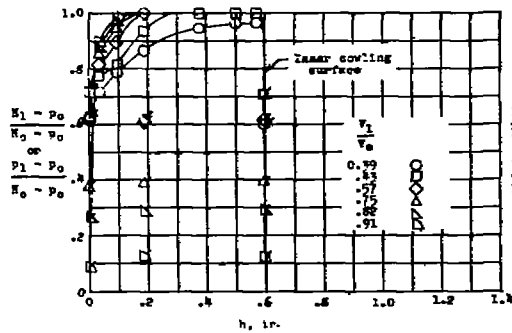
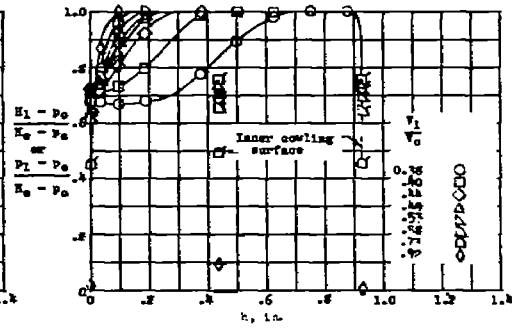


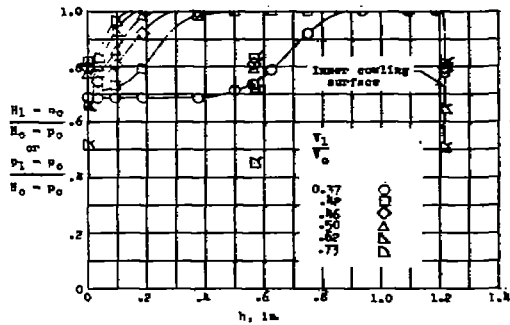
Figure 13.- Effect of propeller shank-spinner juncture configuration on the average impact pressure coefficient at the inlet of the basic cowling. $\alpha = 0^\circ$; $M_0 = 0.79$.



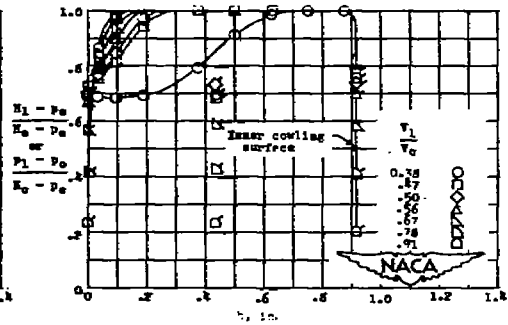
(a) NACA 1-63.8-077.7 cowling,
 $A_d/A_1 = 2.26$.



(b) NACA 1-69.8-077.7 cowling,
 $A_d/A_1 = 1.4$.



(c) NACA 1-75.6-077.7 cowling,
 $A_d/A_1 = 1.0$.



(d) NACA 1-69.8-077.7 cowling,
 $A_d/A_1 = 1.0$.

Figure 14.- Representative total- and static-pressure distributions at the inlet of the several cowling configurations. Propeller removed; $\alpha = 0^\circ$; $M_0 = 0.3$. Flagged symbols indicate static pressures.

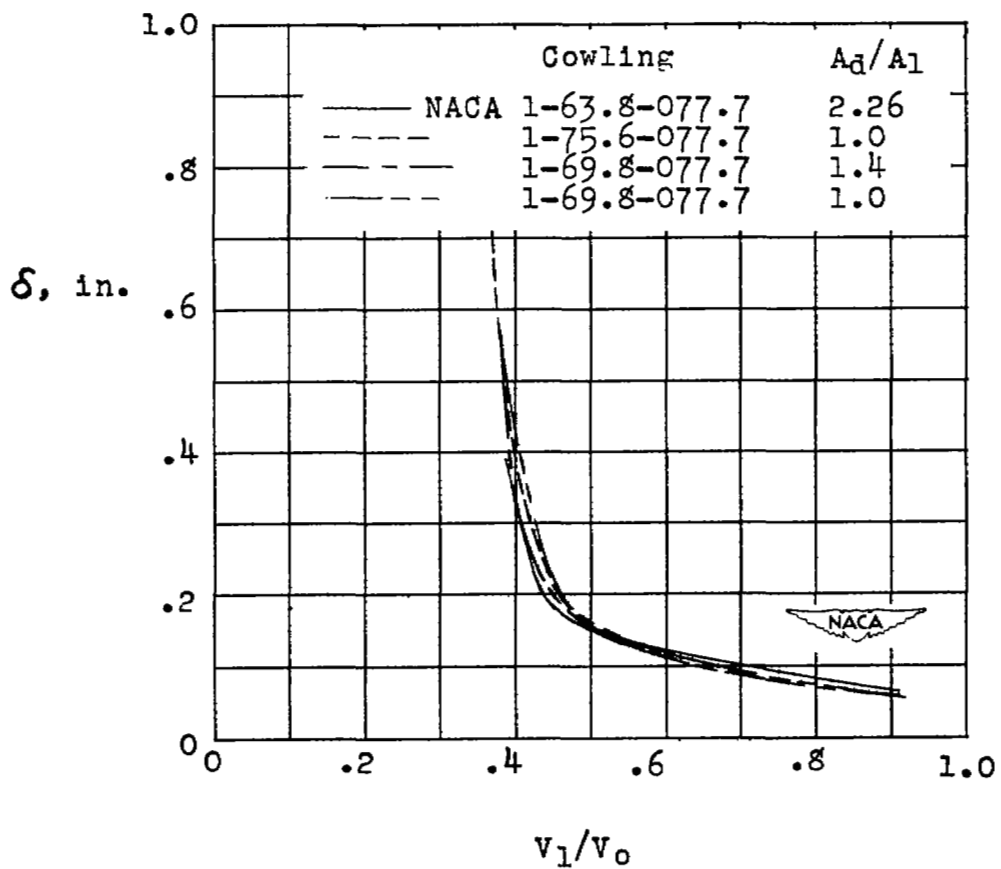


Figure 15.- Effect of inlet-velocity ratio on spinner boundary layer at representative inlet position. Propeller removed; $\alpha = 0^\circ$; $M_0 = 0.3$.

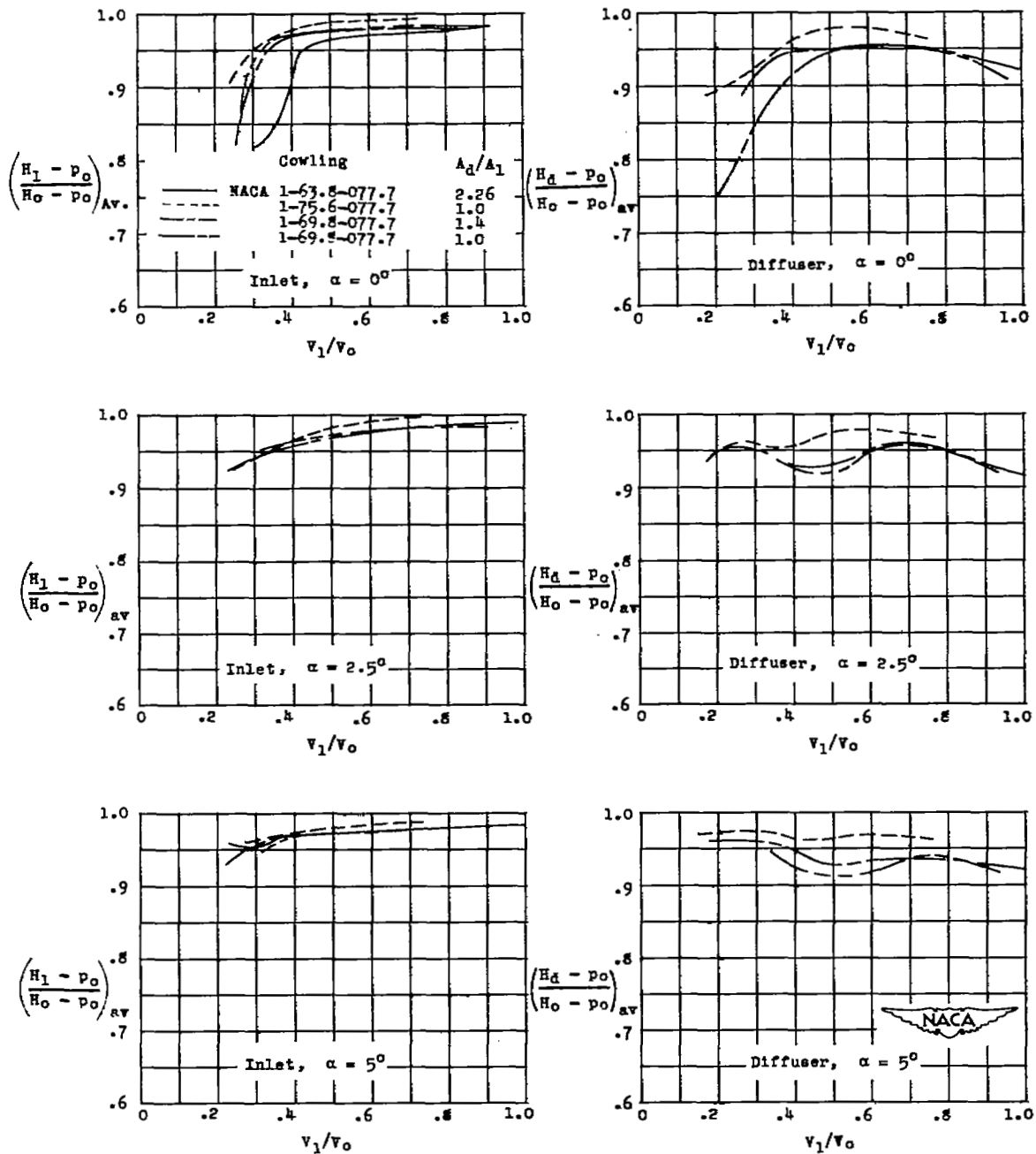


Figure 16.- Effect of inlet-velocity ratio and angle of attack on the average impact pressure coefficient at the inlet and diffuser stations of the several cowling configurations. Propeller removed; $M_o = 0.3$.

SECURITY INFORMATION

NASA Technical Library



3 1176 01436 9954

